ISTANBUL TECHNICAL UNIVERSITY ★ GRADUATE SCHOOL

EXPERIMENTAL INVESTIGATION OF HEAT TRANSFER PERFORMANCE OF FIN-AND-TUBE HEAT EXCHANGERS FOR DRY AND WET CONDITIONS

M.Sc. THESIS

Oguz KILIC

Department of Mechanical Engineering

Heat-Fluid Programme

JUNE 2024

ISTANBUL TECHNICAL UNIVERSITY ★ GRADUATE SCHOOL

EXPERIMENTAL INVESTIGATION OF HEAT TRANSFER PERFORMANCE OF FIN-AND-TUBE HEAT EXCHANGERS FOR DRY AND WET CONDITIONS

M.Sc. THESIS

Oguz KILIC
(503201139)

Department of Mechanical Engineering

Heat-Fluid Programme

Thesis Advisor: Prof. Dr. Mustafa ÖZDEMİR

JUNE 2024

İSTANBUL TEKNİK ÜNİVERSİTESİ ★ LİSANSÜSTÜ EĞİTİM ENSTİTÜSÜ

KANATLI BORULU ISI DEĞİŞTİRİCİLERİNDE ISI TRANSFERİ PERFORMANSININ KURU VE ISLAK KOŞULLARDA DENEYSEL OLARAK İNCELENMESİ

YÜKSEK LİSANS TEZİ

Oğuz Kılıç
(503201139)

Makine Mühendisliği Anabilim Dalı

Isı - Akışkan Programı

Tez Danışmanı: Prof. Dr. Mustafa ÖZDEMİR

HAZİRAN 2024

Oguz KILIC, a M.Sc. student of ITU Graduate School student ID 503201139, successfully defended the thesis entitled "**Experimental Investigation of Heat Transfer Performance of Fin-and-Tube Heat Exchangers For Dry And Wet Conditions**" which he prepared after fulfilling the requirements specified in the associated legislations, before the jury whose signatures are below.

Thesis Advisor :	**Prof. Dr. Mustafa ÖZDEMİR** Istanbul Technical University	.....
Jury Members:	**Prof. Dr. Hakan DEMİR** Yıldız Technical University	.....
	Prof. Dr. Lütfullah KUDDUSİ Istanbul Technical University	.....

Date of Submission : 5 June 2024
Date of Defense : 14 June 2024

To my wife and family,

FOREWORD

I would like to thank my advisor, Prof. Dr. Mustafa OZDEMIR, for all his help and support with this thesis. He has been a great help and I'm really grateful to work with him. I would also like to thank the co-workers at Friterm Inc. for all their help. They were much helpful at every stage of this study. I would like to thank my parents, my brother, and friends for their support. I would also like to thank my wife, she was my biggest supporter in this process.

JUNE 2024

Oğuz KILIÇ
(Mechanical Engineer)

TABLE OF CONTENTS

Page

ABBREVIATIONS

N **:** Row Count

RH **:** Relative Humidity

SYMBOLS

A_0 : External Surface Area [m^2]

A_{fin} : Fin Area [m^2]

A_{tube} : Tube Area [m^2]

A_i : Tube Inner Area [m^2]

b'_r : Slope of the air saturation curved at the mean water temperature [kJ/kgK]

b'_p : Slope between the outside and inside tube surface temperatures [kJ/kgK]

$b'_{wf,p,out}$: Slope of the saturated moist air entalpy curved at the mean water film temperature of the fin surface [kJ/kgK]

b'_{wf} : Slope of the saturated moist air entalpy curved at the mean water film temperature of the outer tube surface [kJ/kgK]

$C_{p,w}$: Specific Heat of Water [kJ/kg]

D_o : Tube Outer Diameter [mm]

D_i : Tube Inner Diameter [mm]

f : Darcy Friction Factor [-]

F_p : Fin Pitch [mm]

F : Correction Factor [-]

G : Mass Flux [kg/m^2s]

h_i : Heat Transfer Coefficient for Tubes [W/m^2K]

h_o : Air Side Heat Transfer Coefficient [$W/m^2 K$]

$h_{o,w}$: Air Side Heat Transfer Coefficient in Wet Conditions [$W/m^2 K$]

$i_{a,i}$: Air Inlet Entalphy [kJ/Kg]

$i_{a,o}$: Air Outlet Entalphy [kJ/Kg]

i : Entalphy [kJ/kg]

$i_{a,m}$: Mean Air Entalphy [kJ/kg]

$i_{r,m}$: Mean Air Entalphy at mean water temperature [kJ/kg]

$i_{a,in}$: Inlet moist air Entalphy [kJ/kg]

$i_{a,out}$: Outlet moist air Entalphy [kJ/kg]

$i_{r,in}$: Saturated moist air entalphy at the inlet water temperature [kJ/kg]

$i_{r,out}$: Saturated moist air entalphy at the outlet water temperature [kJ/kg]

$i_{r,p,in,m}$: Saturated moist air entalphy at the inner surface temperature [kJ/kg]

$i_{r,p,out,m}$: Saturated moist air entalphy at the outer surface temperature [kJ/kg]

j : Colburn Factor[-]

k_{tube} **:** Thermal Conductivity of tube [W/mK]

k_w **:** Thermal Conductivity of water [W/mK]

L **:** Finned Length [mm]

Nu **:** Nussel Number [-]

Pr **:** Prandtl Number [-]

Re **:** Reynolds Number [-]

R_t **:** Total thermal resistance [W/ m^2 K]$^{-1}$

$R_{fouling}$ **:** Fouling resistance [m^2 K/W]

$R_{t,c}$ **:** Thermal Contact Resistance [W/ m^2 K]

$\dot{m}_w$ **:** Mass Flow for Water [kg/s]

$\dot{m}_a$ **:** Mass Flow for Air [kg/s]

St **:** Stanton Number [-]

S_L **:** Longitudinal Pitch [mm]

S_T **:** Transverse Pitch [mm]

T **:** Temperature [ºC]

$T_{w,i}$ **:** Inlet Tempereature of Water [ºC]

$T_{w,o}$ **:** Outlet Tempereature of Water [ºC]

$T_{a,i}$ **:** Inlet Tempereature of Air [ºC]

$T_{a,o}$ **:** Outlet Tempereature of Air [ºC]

$T_{r,p,in,m}$: Inner surface temperature of tube [ºC]

$T_{r,p,out,m}$: Outer surface temperature of tube [ºC]

U_0 **:** Overall Heat Transfer Coefficient [W/ m^2 K]

$U_{0,w}$: Overall Heat Transfer Coefficient [W/ m^2 K]

w : Specific Humidity [kg/kg]

W : Coil Width [mm]

Q : Capacity [kW]

η_0 : Surface Efficiency [-]

η_f : Fin Efficiency [-]

$\eta_{f,wet}$: Fin Efficiency in Wet Conditions [-]

Δi_{lm} : Logaritmic Mean Enthalphy[kJ/Kg]

φ : Adjusment Diameter[mm]

ΔT_{lm} : Logaritmic Mean Temperature[^oC]

ΔP : Pressure Difference[Pa]

LIST OF TABLES

Page

LIST OF FIGURES

Page

EXPERIMENTAL INVESTIGATION OF HEAT TRANSFER PERFORMANCE OF FIN-AND-TUBE HEAT EXCHANGERS FOR DRY AND WET CONDITIONS

SUMMARY

In this study, an experimental study was carried out on fin-and-tube heat exchangers. Fin-and-tube heat exchangers are a type of heat exchanger used for enviroment conditioning in the HVAC indsutry. The most frequently used places are offices, community centres (shopping malls, hospitals, etc.), residences. The common function of these places is that people are actively work in these places. Thermal comfort is required for people to work, live or live more comfortably where they are located. The definition of thermal comfort generally refers to the work of employees in offices in air conditions with ideal temperature, humidity and air flow. Although the limits of temperature, humidity and airflow values in this definition change in different places, the definition itself does not change. Air handling units are systems installed for thermal comfort in places where people are located. Fin-and-tube heat exchangers are one of the most important parts of this system.

Fin-and-tube heat exchangers basically consist of fins and tubes. In order to increase the heat transfer surface, the fins are placed with a determined fin pitch. The tubes are tightly passed through the tube holes in these fins. There are many parameters affecting the heat transfer performance of fin-and-tube heat exchangers. Geometrically, tube arrangement, fin geometry and thickness, tube diameter, tube material are the most significant factor parameters. Air-side inlet conditions of the heat exchanger are also among the parameters affecting the heat transfer performance. In the literature, there are many studies examining the effect of tube side on heat transfer in fin-and-tube heat exchangers and examining the performance of air-side on heat transfer. The results of the studies have provided more comprehensive information about the influence of the fluid in the tube on heat transfer, compared to the effect of the air side on heat transfer performance. Present studies are currently being conducted on the air side.

In fin-and-tube heat exchangers, air is heated or cooled for conditioning. There are studies in the literature where humid air is heated, that is, dry conditions without condensation on the surfaces. There are also studies in the literature about the conditions in which humid air is cooled. In this case, condensation occurs when the fin surface temperature is smaller than the dew point in those conditions, considering the temperature and humidity of the air.

In this thesis, the fin-and-tube heat exchanger was tested under dry and wet conditions. The air temperature is the same in dry and wet conditions. The experiments were carried out on a single heat exchanger with the same number of rows, the same fin spacing and the same geometrical tube arrangement. Air-side inlet relative humidity and air velocity were considered as variable parameters. Experiments were carried out at 90%, 80% ,70% and %30 inlet relative humidity respectively.

KANATLI BORULU ISI DEĞİŞTİRİCİLERİNDE KURU HAVA VE NEMLİ HAVANIN ISI TRANSFERİ PERFORMANSININ DENEYSEL OLARAK İNCELENMESİ

ÖZET

Bu çalışmada kanatlı borulu ısı değiştiriciler üzerinde deneysel bir çalışma yapılmıştır. Kanatlı borulu ısı değiştiricileri iklimlendirme sektöründe ortam şartlandırılması için kullanılan bir ısı değiştirici tipidir. En sık kullanıldığı yerler ofis, toplum merkezleri (alışveriş merkezleri, hastane vb.) , konut gibi yerlerdir. Bu yerlerin ortak özelliği insanların aktif halde bu yerlerde bulunmasıdır. İnsanların bulunduğu yerlerde daha rahat çalışması, bulunması veya yaşaması için termal konfor gereklidir. Termal konfor tanımı genel olarak ofislerde çalışanların ideal sıcaklık, nem ve hava akımının olduğu iklim koşullarında çalışmasını ifade eder. Farklı yerlerde bu tanımdaki sıcaklık, nem ve hava akımı değerlerinin sınırları değişse de tanımın kendisi değişmez. Klima santralleri insanların bulunduğu yerlerdeki termal konfor için kurulmuş sistemlerdir. Kanatlı borulu ısı değiştiricileri bu sistemin en önemli kısımlarından biridir.

Kanatlı borulu ısı değiştiricileri temel olarak lamel ve borudan oluşmaktadır. Isı transfer yüzeyinin arttırmak amacıyla birçok kanadın arka arkaya belirli bir aralıklarla konulması ve düzenli olarak dizilmiş boru demetinin boru kanatların içerisinden sıkı geçmesiyle oluşturulmuş yapılardır. Kanatlı borulu ısı değiştiricilerindeki ısı transferi performansını etkileyen birçok parametre mevcuttur. Geometrik olarak bakıldığında boru dizilimi, kanat geometrisi ve kalınlığı, boru çapı, boru malzemesi en önemli etken parametrelerindendir. Isı değiştiricisinin hava tarafı giriş şartları da ısı transferi performansını etkileyen parametreler arasındandır. Literatürde kanatlı borulu ısı değiştiricilerinde boru içi akışının ısı transferine etkisini ve hava tarafındaki koşulların ısı transferine performansını inceleyen birçok çalışma bulunmaktadır. Yapılan çalışmalar neticesinde, literatürde boru içerisindeki akışın ısı transferine etkisi hava tarafının ısı transfer performansına etkisine kıyasla daha çok kabul edilmiş bilgiler mevcuttur. Hava tarafı ile ilgili çalışmalar hala devam edilmektedir.

Kanatlı borulu ısı değiştiricilerinde hava şartlandırılmak için ısıtılır veya soğutulur. Nemli havanın ısıtıldığı yani yüzeylerde yoğuşma olmayan kuru şartlardaki çalışmalar literatürde mevcuttur. Nemli havanın soğutulduğu durumlar ile ilgili de literatürde çalışmalar mevcuttur. Bu durumda kanat yüzey sıcaklığı, havanın sıcaklığı ve nemi göz önüne alındığında o şartlardaki çiğ noktasından daha küçük olduğu durumlarda yoğuşma meydana gelmektedir.
Bu tez kapsamında, kanatlı borulu ısı değiştiricisinin kuru ve ıslak şartlarda deneyleri yapılmıştır. Kuru şart ve ıslak şartlardaki yapılan deneylerde hava sıcaklığı aynıdır. Deneyler aynı sıra sayısı, aynı kanat aralığı ve aynı geometrik boru dizilimi olmak üzere tek bir ısı değiştiricisi üzerinden yapılmıştır. Hava tarafı giriş bağıl nemi ve hava hızı değişken parametre olarak kabul edilmiştir. Sırası ile %90,%80 ve %70 giriş bağıl neminde deneyler yapılmıştır.

Birinci bölümde tezin amacından ve literatür çalışmalarından bahsedilmiştir. Bu çalışmada, 4 sıralı ve 31.75 x 28 mm tüp düzenine sahip bir kanatlı ve borulu ısı

eşanjörü farklı bağıl nemlerde test edilmiştir. Deneysel çalışmalar yoğuşmasız kuru koşullar ve yoğuşmalı ıslak koşullar için gerçekleştirilmiştir. Tezin amacı, kuru ve ıslak şartlarda yapılan ısı değiştiricisi deneylerinden elde edilen Colburn-j faktörünü literatürde kullanılan korelasyonlarla karşılaştırılmasıdır. Aynı zamanda kanatlı borulu ısı değiştiricileri ile ilgili bilgiler verilmiştir.
Bölüm 2'de ise kanatlı borulu ısı değiştiricilerinin ısı transferi için teorik hesaplaması ile ilgili bilgiler verilmiştir. Elektrik benzeşim metotlarının özeti olarak toplam ısı geçiş katsayısının hem ıslak hem de kuru şartlarda teorik hesaplanması detaylı olarak anlatılmıştır. Kanat verimi ve yüzey verimi kavramlarının yanı sıra hava tarafı ve akışkan tarafı ısı taşınım katsayısının bulunması için literatürde kullanılan örnek korelasyonlar paylaşılmıştır.

Bölüm 3'de tez çalışmasındaki deneysel çalışma anlatılmıştır. Deneysel çalışmanın gerçekleştiği laboratuvar, deney koşulları ile ilgili bilgiler aktarılmıştır. Deneyler sırasında kullanılan kanatlı borulu ısı değiştiricisinin yapısal özellikleri ile ilgili bilgiler verilmiştir. Kuru şartlarda ve ıslak şartlarda deneylerin yapılma sürecini ve deney sonuçları detaylı olarak Bölüm'3 içerisinde paylaşılmıştır.

Bölüm'4 de ise, Bölüm 3 kısmında deneysel verilerden alınan bilgiler kullanılarak deneysel çalışmadaki boyutlu bir parametre olan ısı taşınım katsayısı değeri elde edilmiştir. Elde edilen ısı taşınım katsayısı verisi hem kuru şart hem de ıslak şart içinde kullanılarak boyutsuz bir parametre olan Colburn-J faktörü bulunmuştur.

Bölüm 5 içerisinde ise yapılan çalışmanın bir özeti ve sonuçların değerlendirilmesi yapılmıştır.

Kuru şartlardaki testler literatürdekiler ile karşılaştırılırken ıslak şartlardaki testler kendi içinde değerlendirilmiştir. Sonuç kısmında ise kuru ve ıslak şartlardaki deney sonuçları kendi içerisinde yorumlanmıştır.

Kuru koşullarda, hava hızı arttıkça, ısıl kapasite ve hava tarafı basınç kaybı değeri artmaktadır. Hava hızı iki katına çıktığında hava tarafı basınç kaybı değeri 2.85 kat artmaktadır.

Kuru koşullarda, Reynolds sayısı arttıkça kanatçık verimi düşmektedir. Reynolds sayısı iki katına çıktığında kanatçık verimi %6.2 oranında azalmaktadır.

Reynolds sayısı arttığında Colburn j-faktörü azalmaktadır. Isı transfer katsayısı Colburn j-faktörünün tamamen tersi bir davranış gösterir. Reynolds sayısı arttıkça ısı transfer katsayısı da artar. Reynolds sayısı iki katına çıktığında Colburn j-faktörü %30.5 oranında azalırken ısı transfer katsayısı değeri %35.5 oranında artmaktadır.

Deneysel sonuçlardan elde edilen ısı transfer katsayısı ve Colburn j faktörü değerleri literatürde VDI Heat Atlas (2010) korelasyonuna benzemektedir. Düşük Reynolds sayılarında %10'luk bir fark varken, Reynolds sayısı arttıkça bu fark %1'e düşmüştür. Rich (1973) korelasyonunda ise düşük Reynolds sayılarında sonuçlar oldukça benzer iken Reynolds sayısı arttıkça sonuçların ayrıştığı gözlemlenmiştir.

Islak koşullarda aynı Reynolds sayısı ve farklı bağıl nemlerde sonuçlar %3 ile %10 arasında değişmektedir.

Kuru ve ıslak koşulların hava tarafı basınç kaybı değerleri aynı Reynolds sayısında karşılaştırıldığında, minimum %56 ve maksimum %80 fark ile ortalama %71 fark vardır.

Isı transfer katsayısı ve Colburn j-faktörü değerleri birbiriyle uyumludur. Islak ve kuru şartlarda ısı transfer katsayısı değeri düşük bağıl nemde yaklaşık 2.5 kat daha fazla iken, %90 bağıl nemde bu oran 3.1 kata kadar çıkmaktadır.

1. INTRODUCTION

Heat transfer is the process by which thermal energy is transferred between two substances, such as fluids. This change in temperature, known as heat transfer, always occurs from a high temperature to a low temperature by conduction, convection or radiation.

Heat transfer is the process by which thermal energy is transferred between two substances, such as fluids. This change in temperature, known as heat transfer, always occurs from a high temperature to a low temperature by conduction, convection or radiation.

Heat exchangers are mechanical devices designed to enable thermal energy transfer between two or more fluids at different temperatures. These devices are commonly known as heat exchangers, though they may have other names depending on their specific application. There are many types of heat exchangers used in industry, typically involving the temperature change of one fluid through the cooling or heating effect of another. In some cases, this energy transfer can also cause simultaneous evaporation or condensation.

In the refrigeration industry, condensers and evaporators are among the most common types of heat exchangers. Beyond refrigeration, heat exchangers are widely used in air conditioning systems, heat recovery systems, and process control systems. They can be classified based on whether the fluids are in direct contact. In some designs, the fluids directly contact each other to transfer thermal energy, while in others, a separating wall prevents mixing. Many heat exchangers use a heat transfer wall to separate the fluids, representing a type of non-direct heat transfer or regenerative heat exchanger. The most common types of heat exchangers include tubular heat exchangers, automobile radiators, condensers, evaporators, air preheaters, and cooling towers. [3]

The tests carried out as part of this thesis relate to fin and tube heat exchangers. These devices consist of two primary components: fins and tubes. The tube material is usually

copper or aluminium. Copper is the most commonly utilised material due to its high thermal conductivity, which has a beneficial impact on heat transfer.

The surface area of the battery can be expanded in order to enhance the heat transfer with the fluid and air that circulate within the coil. This surface area expansion is achieved by the placement of fins on the tube surfaces. The type of fin model used affects the performance of the heat exchanger. Consequently, a variety of fin models are utilised in the heat exchanger industry. Pure aluminium is typically utilised as fin material. In instances where ambient conditions are harsh (corrosive, humid, etc.), it is preferable to utilise hydrophilic-coated aluminium or epoxy-coated aluminium.

As fin-and-tube heat exchangers are part of a larger system, it is necessary to distribute the fluid entering the system into the tubes. This is achieved through the use of manifolds. The fluid that will pass through the tubes within the heat exchanger is either liquid or gas. The external fluid is either dry air or moist air containing water vapour. In heat exchangers, the temperature of the external fluid determines whether the air is cooled or heated after the process is complete. In industry, these heat exchangers are also referred to as coils. In the thesis, a cooling coil is employed through which water passes as a fluid.

The first chapter sets out the aim of the thesis and literature studies review. It also provides information about finned tube heat exchangers.

Chapter 2 explains the theoretical analysis of heat transfer calculation for fin-and-tube heat exchangers.

In Chapter 4, the heat transfer coefficient value, which is a dimensional parameter in the experimental study, was obtained by using the information obtained from the experimental data in Chapter 3. The Colburn j-factor was found by using the heat transfer coefficient obtained for both dry and wet conditions.

In the 5th section, the results of the experiments were interpreted. The graph illustrates the comparison of dry and wet conditions.

1.1 Purpose of Thesis

The objective of this thesis is to examine the thermal performance of a fin-and-tube heat exchanger with a 31.75 mm x 28 mm tube arrangement, which has not been

extensively researched in the literature. These experiments was achieved under different ambient conditions. The fin-and-tube heat exchanger was analysed according to the presence or absence of condensation inside the fin-and-tube heat exchanger. In the case where no condensation is present, a comparison is made with the correlations that are suitable for the heat exchanger geometry and ambient conditions in the thesis study, as well as those in the literature. A comparison was then made between the results in the relevant correlation and the experimental results. Given the absence of comparable studies on condensation in the existing literature, the objective of this study is to serve as a reference point for future research and to enable comparisons within the same study.

1.2 Literature Review

The most commonly used fin arrangement in fin-and-tube heat exchangers is the flat fin model. Studies have been carried out for years to compare the heat transfer performance and friction factor of round tube heat exchangers in the flat fin model. There are studies in the literature not only for Plain-fin, but also for straight tube and louver, wavy model. All these studies can basically be analysed under two different headings as dry surface and wet surface. For dry surfaces, the most comprehensive studies were carried out by Rich D.G. [24] in a 4-row finned tube heat exchanger and concluded that heat transfer and friction factor are independent of fin pitch. Rich [18] conducted experiments on different heat exchangers with 1-6 rows. Rich D.G. conducted experiments with longitudinal and transverse tube pitches were 27.5 and 31.75 mm, respectively and tube diameter 13.34 mm. Mcquiston (1980) proposed the first general correlation for plain fin pattern based on his test results of five test samples (Fp = 1:81-6:35 mm, D_o = 9:96 mm, S_L = 22 mm, S_T 25:4 mm and N = 4). The root-mean-square error of the correlation obtained in this study, which is valid for N≥4, is 7.3% for heat transfer coefficient and 7.8% for friction factor. The prediction value of Gray et al.[16] correlation is more reasonable for larger tube diameters and longer tube layouts. In their study, they stated that j-correlation is independent of fin pitch, but for f -correlation, f factor increases as fin pitch decreases.

Wang (1996) conducted experiments using 15 different specimens in his study. In this study, he examined the effect of several geometry parameters such as row number, fin spacing and fin thickness (D_o = 10.3 mm, S_L = 22 mm, S_T 25:4 mm mm and N = 2-6.)

He reported that fin pitch has a negligible effect on the heat transport coefficient and that the colburn j-factor and friction factor are independent of fin thickness.

For wet surfaces, many studies have investigated fully wet surfaces. Fully wet means that temperature is lower than the dew point throughout the whole fin surfaces. Partial condensation studies are available in the literature, but most researchers avoid these studies. The reason for this is that the fin efficiency on the dry and wet surface must be calculated and evaluated separately. However, the movement of droplets in condensation makes it very difficult to determine this visually [19]. McQuiston [12] found an increase of both heat transfer and friction under wet conditions and reported that j is higher for dropwise condensation than filmwise condensation. Many other investigators agree on the increase of f under wet conditions, but there is not uniform agreement that j increases under wet conditions. Wang et. Al [5] has found that colburn j-factor decreases for $Re_{Do} \leq 2000$ but colburn j-factor is almost same or a slightly higher than dry conditions for $Re_{Do} \geq 2000$. This study also claim that fin pitch has negligible effect on colburn j-factor and friction factor under wet conditions. Wang et al. [5] reported that the effect of relative humidity on friction factor is negligible for plain-fin, round-tube heat exchangers under fully wet conditions, and that colburn j-factor is almost independent of relative humidity.

2. THEORITICAL ANALYSIS OF HEAT TRANSFER OF FIN-AND-TUBE HEAT EXCHANGER

This section provides information about the theoretical calculation of fin-and-tube heat exchangers.

2.1 Heat Capacity Calculation

The mathematical equations that describe the heat transfer calculation of these heat exchangers, as presented in Chapter 2.[10] The equation for the energy conservation of the air and fluid sides is written as follows.

$$Q = \dot{m}_a (i_{a,i} - i_{a,o}) \tag{2.1}$$

$$Q = \dot{m}_w C_{p,w} (T_{w,o} - T_{w,i}) \tag{2.2}$$

In Equations 2.1 and 2.2, the kinetic and potential energy changes in the inlet and outlet sections were not considered. The mean values of main properties such as enthalpy and temperature are taken into account. The enthalpies in equation 2.1 represent the average enthalpies of the air-water vapour mixture per dry air flow rate. The average mixture enthalpies can be calculated in accordance with equation 2.3, or the psychrometric diagram can be read.

$$i_a = 1.005T + w(2500.9 + 1.82T) \tag{2.3}$$

In this context, the symbol T represents temperature and is expressed in degrees Celsius (°C). The heat transfer between two fluids is also calculated by the logarithmic temperature difference. The logarithmic temperature difference is used as the basis for the formula in equation 2.4.

$$Q = U_0 A_0 \Delta T_{lm} F \tag{2.4}$$

In Equation 2.4, the following variables are defined: U_0 is the total heat transfer coefficient, A_0 is the total air side surface area, ΔT_{lm} is the logarithmic temperature difference, and F represents the correction factor.

If the heat loss from the outer parts of the heat exchanger is neglected, the thermal capacity (Q) value in equations 2.1, 2.2 and 2.4 should be equal to each other.

2.2 Logaritmic Temperature Difference

It is not the case that the temperature difference between two different temperature fluids in the heat exchanger remains constant. Consequently, the calculation of logarithmic temperature differences plays an important role in the estimation of thermal capacity. The mathematical description of the logarithmic temperature difference is illustrated in Equation 2.6 below. This description is obtained by dividing the heat exchanger into cells, which facilitates the solution and allows for the calculation of the energy balance in each cell.

$$\Delta T_{lm} = \frac{\Delta T_1 - \Delta T_2}{\ln \frac{\Delta T_1}{\Delta T_2}} \tag{2.6}$$

The calculations of ΔT1 and ΔT2 in the logarithmic temperature difference are dependent on the direction of flow. The logarithmic temperature difference calculations of ΔT1 and ΔT2 differ according to the direction of flow, whether in a counter or parallel flow.

For counter flow;

$$\Delta T_1 = T_{a,i} - T_{w,o} \qquad \Delta T_2 = T_{a,o} - T_{w,i} \tag{2.6}$$

For parallel flow

$$\Delta T_1 = T_{a,i} - T_{w,i} \qquad \Delta T_2 = T_{a,o} - T_{w,o} \tag{2.7}$$

2.3 Surface Area Calculation

In order to correctly define the area of the cooling coil, it is necessary to make a proper definition and calculation of the relevant parameters. The following paragraphs set out the definitions and calculations that are required.

$$L_{total} = LN_{row}N_{tube} \tag{2.8}$$

$$W = N_{row}BS_L \tag{2.9}$$

$$H = N_{tube}BS_T \tag{2.10}$$

$$A_{front} = LH \tag{2.11}$$

Total Fin Area

$$A_{fin} = 2(LH - N_{c,d}N_{tube}N_{row} + N_{tube}BS_T\delta)N_{fin} \tag{2.12}$$

Total Tube Outer Surface Area

$$A_{tube} = (\pi D_o L - \pi D_o \delta \frac{L}{F_p} - 1)N_{tube}N_{tube} \tag{2.13}$$

Total Tube Inner Surface Area

$$A_{tube,i} = (\pi D_i L)N_{tube}N_{tube} \tag{2.14}$$

Total Surface Area

$$A_0 = A_{fin} + A_{tube} \tag{2.15}$$

2.4 Overall Heat Transfer Coefficient

In heat exchangers, the overall heat transfer coefficient is one of the most crucial parameters influencing heat transfer performance. The most basics and uncertain

parameter in any heat exchanger is the total heat transfer coefficient. The total heat transfer coefficient is calculated with the help of thermal resistances. Considering the contact resistance and fouling factors, the equation is given in its most general form in Equation 2.16. [9]

$$\frac{1}{U_0 A_0} = \frac{1}{R_t} = \frac{1}{h_i A_i} + \frac{\ln(\frac{D_o}{D_i})}{2\pi k_{tube} L} + \frac{1}{h_o A_0 \eta_0} + \frac{1}{R_{t,c}} + \frac{1}{R_{fouling}} \tag{2.16}$$

R_t expression is total thermal resistance.

$$R_t = R_i + R_t + R_o + R_f + R_c = \frac{1}{h_i A_i} + \frac{\ln(\frac{D_o}{D_i})}{2\pi k_{tube} L} + \frac{1}{h_o A_0 \eta_0} + \frac{1}{R_{t,c}} + \frac{1}{R_{fouling}} \tag{2.17}$$

$$R_i = \frac{1}{h_i A_i} \tag{2.18}$$

$$R_t = \frac{\ln(\frac{D_o}{D_i})}{2\pi k_{tube} L} \tag{2.19}$$

$$R_o = \frac{1}{h_o A_0 \eta_0} \tag{2.20}$$

h_i is the coefficient of heat transfer R_i in the tube in the resistance. Area is the area of the tube inner diameter. R_t represents the tube thermal resistance. R_o is the thermal resistance of the air side against heat transfer. h_o is the air side heat transfer coefficient, A_o is the total surface area of the air side, η_o ise is the surface efficiency.

This thesis also examines the influence of condensation on the total heat transfer coefficient during wet coil tests. It refers to Section 2.5 for a comprehensive explanation of the methodology employed in calculating the total heat transfer coefficient for the wet coil for the wet coil is explained in detail in Section 2.5.

2.4.1 Heat transfer coefficient of fluid side

In order to calculate the total heat transfer coefficient, it is necessary to determine the unknown expressions in equation 2.16. h_i represents the heat transfer coefficient of the fluid side in the tube. In the study presented in this thesis, it is assumed that the heat transfer coefficient in the tube is constant. This is because the water flow rate is not variable. The Gnielinski correlation is employed to obtain the heat transfer coefficient. In the Gnielinski correlation, different equations are used according to the flow characteristics. The flow characteristic is determined by the Reynolds number. In the calculation of the Reynolds number, the inner diameter of the tube is accepted as the characteristic length. The transition region between Re=2100 and Re=2300 is accepted by Gnielinski. Fully developed turbulent flow is valid for Re≥10000. [20] The correlation of Gnielinski correlation in different characteristic cases is given below. The following correlation is recommended for the flow in the tube when the Reynolds number is greater than 10000.

$$Nu = \frac{\frac{f}{8}\mathrm{Re}\,\mathrm{Pr}(T)}{1+12.7\frac{f}{8}^{0.5}(\mathrm{Pr}(T)^{2/3}-1)} + \left[1+\left(\frac{d_i}{l}\right)^{2/3}\right] \tag{2.21}$$

$$f = (1.8\ln(\mathrm{Re}) - 1.5)^{-2} \tag{2.22}$$

In the case of a flow in the transition zone, the equation given in Equation 2.23 is to be preferred.

$$Nu = (1-\gamma)Nu_{lam,2300} + \gamma Nu_{turn,10000} \tag{2.23}$$

$$\gamma = \frac{\mathrm{Re}-2300}{10000-2300} \tag{2.24}$$

In the event that the Nusselt number and Reynolds number are known, the heat transfer coefficient in the tube can be calculated in accordance with the equation presented in Equation 2.25.

$$Nu = \frac{h_i D_i}{k_w} \qquad h_i = \frac{Nuk_w}{D_i} \tag{2.25}$$

The heat transfer coefficient can be employed to express the convection resistance in the total heat transfer coefficient equation.

2.4.2 Heat transfer coefficient of air-side in dry condition

In order to identify the air-side correlation in dry conditions, a fin correlation was implemented. In order to achieve this objective, the *VDI Heat Atlas*. (2010) correlation was employed.

$$Nu = 0.38\,\mathrm{Re}_{air}^{\,0.6}\left[\frac{A_0}{A_{t,b}}\right]^{-0.15}\mathrm{Pr}_a(T_{avg})^{1/3} \tag{2.26}$$

$$h_a = \frac{Nu_{\,a}k_a(T_{avg})}{D_o} \tag{2.27}$$

The correlations presented in the VDI Heat Atlas [13] vary according to the number of rows. Moreover, different correlations are employed according to whether the tube arrangement is in-line or staggered. The correlation defined in Equation 2.26 is applicable to a staggered tube arrangement. Equation 2.28 provides a general correlation for the air-side Nusselt number.

$$Nu = C\,\mathrm{Re}_{air}^{\,0.6}\left[\frac{A_0}{A_{t,b}}\right]^{-0.15}\mathrm{Pr}_a(T_{avg})^{1/3} \tag{2.28}$$

Table 2.1 : Air-side Nusselt number correlation coefficient.

Coil Row Count	Staggared Arrangement	Inline Arrangement
2	C=0.33	C=0.20
3	C=0.36	C=0.36

2.4.3 Fin efficiency and surface efficiency calculations

Fin efficiency is one of the important parameters in thermal performance. The highest temperature difference for convection is the temperature difference between the temperature at the point where the fin contacts the tube, called the base temperature, and the fluid. Therefore, the highest value of the thermal energy emitted by the fin is realised when the entire surface of the fin is at the base temperature.

$$\eta_f = \frac{q_f}{q_{\max}} = \frac{q_f}{hA_f\theta_b} \tag{2.29}$$

$$\eta_f = \frac{\tanh(mL)}{mL} \tag{2.30}$$

The flat-fin model will be the focus of this thesis. Additionally, wavy, louvred and circular type fins can be utilised in fin-and-tube heat exchangers. The fin efficiency calculation is necessary for the determination of the air-side heat transfer coefficient, or, in theory, for the total heat transfer coefficient calculation. In order to calculate the efficiency of the fins, the efficiency formula given for the flat fin model in the VDI Heat Atlas must be employed [13].

The efficiency of the fin for the flat-fin model is described in Equation 2.31.

$$\eta_f = \frac{\tanh(X)}{X} \tag{2.31}$$

$$X = \varphi\frac{D_o}{2}\sqrt{\frac{2h_o}{k_{tube}\delta}} \tag{2.32}$$

$$\varphi' = 1.28\frac{b_f}{d_o}\sqrt{\frac{l_f}{b_f} - 0.2} \quad , \varphi = (\varphi' - 1)(1 + 0.35\ln(\varphi')) \tag{2.33}$$

The term "fin surface efficiency" is also used to refer to the total surface efficiency. In contrast to fin efficiency, which provides insight into the thermal behaviour of a fin, total surface efficiency is a parameter that offers a more comprehensive understanding of the thermal behaviour. This parameter indicates the thermal behaviour of the surface of the tube arrangement on which a fin array is placed.

$$\eta_0 = 1 - \frac{A_f}{A_0}\left(1 - \eta_f\right) \tag{2.34}$$

2.5 Overall Heat Transfer Coefficient for Wet Conditions

Considering the ambient conditions in the cooling coil, the air with high relative humidity is cooled when it passes through the heat exchanger. In case of cooling the humid air, when the fin surface temperature cooled below the dew point temperature of the air, the water vapour in it will condense and turn into liquid phase. In the tests carried out in wet conditions within the scope of this thesis, it is assumed that the fin surface of the heat exchanger where the experimental work is carried out is completely wet, that is, even the highest temperature in the fin-and-tube heat exchanger is lower than the dew point temperature of the air. In case of condensation, heat transfer and mass transfer occur together. Condensation can occur in two different ways as liquid film condensation and droplet condensation on the surface. In droplet condensation, condensed water vapour particles remain as droplets instead of forming a film layer on the surface. These water droplets that later merge can show a flow like a film layer. The heat transfer equation for wet conditions is given in 2.35 below. $U_{0,w}$ value is the overall heat transfer coefficient used in the wet condition unlike the equation in the dry condition. At the same time, logarithmic enthalpy difference is written instead of logarithmic temperature difference. The name of this method is referred to as Threlkeld method in the literature. [21]

$$Q = U_{0,w} A_0 \Delta i_{lm} \tag{2.35}$$

$$U_{0,w} = \frac{Q}{\Delta i_m A_0} \tag{2.36}$$

The Threlkeld method, as described in Equation 2.37, was achieved for the calculation of the overall heat transfer coefficient.

$$\frac{1}{U_{0,w}A_0}=\frac{1}{R_t}=\frac{b'_r}{h_iA_i}+\frac{b'_p\ln(\frac{D_o}{D_i})}{2\pi k_{tube}L}+\frac{1}{h_{o,w}\left[\frac{A_{p,o}}{b'_{wf,p,out}}+\frac{A_f\,\eta_{f,wet}}{b'_{wf}}\right]} \tag{2.37}$$

While the calculation is based on the logarithmic temperature difference in dry conditions, the enthalpy difference is taken into consideration in wet conditions. In the following calculation, the logarithmic enthalpy difference is defined according to Bump (1963) and Meyers (1967). $i_{a,m}$ represents the average air enthalpy and $i_{r,m}$ is the average water temperature at saturated air temperature.

$$\Delta i_m=i_{a,m}-i_{r,m} \tag{2.38}$$

The expansion of the two enthalpy values, which have been defined above, is illustrated in equations 2.39 and 2.40.[25]

$$i_{a,m}=i_{a,in}+\frac{i_{a,in}-i_{a,out}}{\ln\left(\frac{i_{a,in}-i_{r,out}}{i_{a,out}-i_{r,in}}\right)}-\frac{\left(i_{a,in}-i_{a,out}\right).\left(i_{a,in}-i_{r,out}\right)}{\left(i_{a,in}-i_{r,out}\right).\left(i_{a,out}-i_{r,in}\right)} \tag{2.39}$$

$$i_{r,m}=i_{r,out}+\frac{i_{r,out}-i_{r,in}}{\ln\left(\frac{i_{a,in}-i_{r,out}}{i_{a,out}-i_{r,in}}\right)}-\frac{\left(i_{r,out}-i_{r,in}\right).\left(i_{a,in}-i_{r,out}\right)}{\left(i_{a,in}-i_{r,out}\right).\left(i_{a,out}-i_{r,in}\right)} \tag{2.40}$$

In the theoretical analysis of wet conditions, it can be observed that there are thermal resistances that are similar to those observed in dry conditions. Gnielinski correlation is used as the heat transfer coefficient on the tube side as in dry conditions. In contrast to the dry conditions, the tube metal resistance and convection thermal resistance are multiplied by specific heats that are specific to wet conditions. The b'_r b'_p , $b'_{wf,p,out}$ b'_{wf} values of the coefficients are used in the calculation of thermal resistance. The calculation of fin efficiency and total surface efficiency is applicable to both dry and wet conditions. In the case of calculating fin efficiency for wet conditions, the

expression h_o in Equation 2.36 is transformed into $h_{o,w}$, which is employed as the heat transfer coefficient value calculated for wet conditions. In this case, the fin efficiency in wet conditions is designated as $\eta_{f,w}$. It has been demonstrated that the heat transfer coefficient in wet conditions can be 2.5-3 times higher than in dry conditions. Consequently, the efficiency of the fin is significantly reduced. In Chapters 3 and 4, the Reynolds number-dependent fin efficiency graphs for both wet and dry conditions was presented.

2.5.1 Heat transfer coefficient correlation for wet conditions in coils

There are numerous studies and correlations in the literature on wet coils. The correlation in the study published by Wang et al. (1997) is shown below. In the study, Colburn j-factor correlation is given instead of Nusselt number. It is essential to calculate the heat transfer coefficient according to the Colburn J-factor correlation. In Equation 2.41, the correlation in the compatible study for the staggered tube arrangement of 4 rows is written.

$$j = 0.2977 \mathrm{Re}_{air}^{-0.364} \left[\frac{A_0}{A_{\min}} \right]^{-0.168} \tag{2.41}$$

$$h_o = \frac{jG_a Cp_a}{\mathrm{Pr}_a^{2/3}} \tag{2.42}$$

3. EXPERIMENTAL STUDY

In this chapter, the experimental apparatus, the measuring devices used in the experimental setup and the details of all experimental studies carried out in this thesis are described.

3.1 Test Apparatus

Within the scope of this thesis, a fin-and-tube heat exchanger manufactured by Friterm INC. and it was tested under both wet and dry conditions in the laboratory of Friterm R&D Centre. Friterm test laboratory consists of two separate rooms. One of these rooms is used as a conditioning room, while the other is used as a calorimetric room. The conditioning room is where the products are tested in the laboratory without using a fan. Cooling coil tests are also carried out in the conditioning room. The figure 3.1 below shows a wide perspective view of the conditioning room.

Figure 3.1 : Conditioning room.

Figure 3.2 shows two rooms inside the Friterm test laboratory. On the right is the calorimetric room, where fan products such as evaporators and condensers are tested. The room on the left side is where coil tests are carried out. This is also the location where the thesis study was conducted. In Figure 3.2, number 1 represents the place where the coil is placed. The coils are tested there. The image number 2 in the figure is the mixing room, which is the point where the air passing through the coil exits. The

room where the air flow rate is measured is showed by number 3. Number 4 shows the air handling unit.

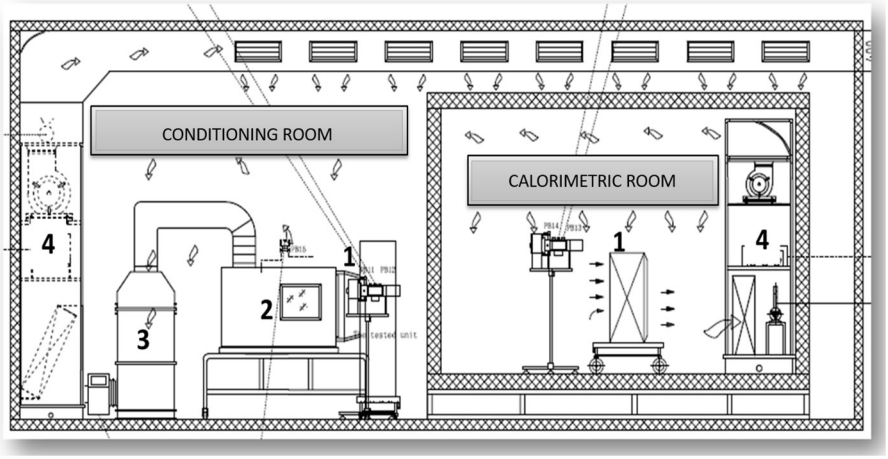

Figure 3.2 : Friterm test laboratory schematic view.

The product to be tested is placed within the air duct. The nozzles allow for the adjustment of the air flow rate. By simply opening and closing them allows for the desired air flow rate to pass through the coil. An air sampler is placed in front of the coil, which is completely insulated and will not be affected by the heat transfer in the external environment. Figure 3.3 illustrates the 35 distinct points in the air sampler. The air is collected from these points and transported to the location idenitifed in Figure 3.2, where a temperature and humidity sensor is located in order to regulate the inlet conditions.

Figure 3.3 : Air sampler.

Figure 3.4 : This is the place where the inlet air properties is measured after collected by the air sampler.

The temperature and relative humidity of the air inlet side are measured as well as the inlet temperature and flow rate of the fluid side are controlled. The temperature control on the fluid side is carried out with temperature sensors placed at the connection points, while the water flow rate control is carried out with the help of a flowmeter. We measure the pressure loss on the air and fluid sides using pressure difference sensors. Once the inlet conditions of the air and fluid sides have reached the desired values, it is advisable to wait for the test to stabilise. The tests are evaluated for equilibrium according to the ASHRAE standards definition of thermal balance. In the test laboratories using the air-enthalpy method, the thermal capacity of the water side and the thermal capacity of the air side are measured separately. The difference between these two capacities is the thermal balance. ASHRAE standards require that the thermal balance be reduced to below 5%. This presented study continues until the thermal balance is reduced to 5% or below. The humidity and temperature sensors are located at the outlet of the coil and the values for the outlet side of the air side was read.

Figure 3.5 : Air outlet part of test apparatus.

The test sample is a cooling coil, and therefore it is evident that the air outlet temperature is cooler than the air inlet temperature of the coil. It is necessary to back the outgoing air to inlet conditions and release it into the room. The outgoing air from the coil is transferred to the air handling unit via fully insulated tubes (see Figure 3.4). The heaters in the air handling unit adjust the air temperature to the desired inlet air temperature and send it to the room. As the air is heated, its relative humidity value decreases. In the event that the humidity level of the environment is below the desired humidity, humidifiers are employed to increase the humidity. The reconditioned air is then returned to the room.

Figure 3.6 : Fully insulated pipes**.**

There are some limitations in the test conditions of the conditioning room. The conditions of the coil to be tested were calculated in advance with FRTCoils® software. It has been checked whether the results are suitable for the test to be carried out under conditioning room conditions. Table 1. below shows the air and water side limits and the capacity limits of the conditioning room.

Table 3.1 : Conditioning room test limits

Limitation Parameters	Values Range
Max. Heating And Cooling Coil Capacity	20 kW
Dry Bulb Temperature	0°C-45°C
Relative Humidity	20-100%
Refrigerants Type	Water
Max. Air Flow	7.500 m^3/h

3.2 Test Apparatus Measurement Devices

The tests were carried out in dry and wet conditions in the conditioning room, and the results obtained were temperature, relative humidity, air flow rate, fluid flow rate and pressure loss data. This chapter explains where and why measurement devices are used and the uncertainties of measurements devices.

PT100® Temperature Sensor: The air inlet temperature was measured at the inlet air temperature sensor location with the air sampler. The outlet air temperature was measured with the temperature sensor located at the outlet of the coil. The PT100® temperature sensor device has an uncertainty of ± 0.1 °C.

Figure 3.7 : The inlet air temperature sensor PT100® is located here.

T-type Thermocouple: The T-type thermocouple was used to measure the surface temperature of the fin. It was used because the surface temperature and dew point temperature are compared in high relative humidity tests, and it is necessary to make comments about where condensation will occur on the fin. The T-type thermocouple was used in three pieces in the test installation. The thermocouple were placed diagonally on the front surface of the test coil, as shown in Figure 3.4. The uncertainty of the T-type thermocouple is ±1°C.

Figure 3.8 : T-type thermocouple placed.

Humidity Sensor: The Galltec® humidity sensor is used to measure the relative humidity at the air inlet and outlet. In order to measure the relative humidity of the air inlet, the Galltec® humidity sensor collects the air from 35 different points with the help of an air sampler and transmits it to the relative humidity sensor, such as the temperature sensor. The relative humidity at the outlet is measured by the humidity sensor located at the outlet part of the experiment apparatus. There are two humidity sensors in the experiment apparatus.

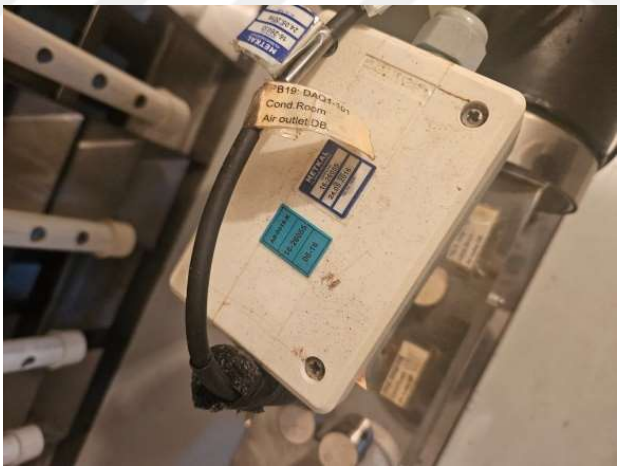

Figure 3.9 : Galltec® humidity sensor.

Flowmeter: During the coil tests, the mass flow rate of the water side was kept constant. The mass flow rate was controlled by a YOKOGAWA digital flowmeter.

Figure 3.10 : Fluid side flowmeter.

Air Volumetric Flow Nozzle: The air flow rate in the test installation is adjusted using nozzles, which are designed to regulate the airflow. Four different diameter nozzles are used. The nozzles, with diameters of 90 mm, 110 mm, 150 mm and 180 mm, respectively, are opened in accordance with the air flow rate. The 90 mm diameter nozzle is always in an open state. The nozzle is opened according to the desired air velocity and made suitable for the experimental conditions.

Figure 3.11 : Nozzles for air volumetric flow**.**

It is essential to ensure that the system achieves thermal balance within the specified test conditions during the test studies. The results of the measuring instruments described above can be controlled in two ways. The first method is the laboratory control panel. The instantaneous values of the sensors in the laboratory can be read on the control panel screen.

Figure 3.12 : Laboratory control panel.

Another method is the utilisation of LabVIEW software. In addition to the average values of the results, measurements can be taken at desired intervals with LabVIEW software. At the same time, the thermal balance expression in the LabVIEW results is employed to ascertain whether the system has reached balanced. Figure 3.9 illustrates the output of the LabVIEW software as an example.

Coil type	Cooling	Project no		Model name	friterm
Order no	2023/4607-01-001	Test no		Fan model	
Software capacity		Software dPfluid		Geometry	F32x28-12 F S
NTxNRxNC	28x4x14	Length x Fin pitch	750x2.5	TT & FT	0.32x0.12

Cold Water_ Bare Coil(Cooling) — Nozzles 80 ◉ 110 ◉ 150 ◉ 150 ◉ 189 ○

Condenser InletTemp.	0 ℃	Condenser InletTemp.	0 ℃
Condenser InletTemp.	0 ℃	Condenser InletTemp.	0 ℃
Condenser InletTemp.	0 ℃	Condenser InletTemp.	0 ℃
Condenser InletTemp.	0 ℃	Condenser InletTemp.	0 ℃

	Unit	1	2	3	4	AVG.
Cond. Room Air Inlet DB	℃	20.00	20.01	20.01	20.00	20.00
Cond. Room Air Inlet DP	℃	14.24	14.53	14.42	14.41	14.40
Cond. Room Air Outlet DB	℃	12.87	12.87	12.87	12.88	12.87
Cond. Room Air Outlet DP	℃	12.87	12.87	12.87	12.88	12.87
Temp. Before Nozzles	℃	13.37	13.35	13.36	13.37	13.36
Inlet Relative Humidity	%	69.27	70.54	70.07	70.07	69.99
Air side pressure drop	Pa	36.87	36.83	36.80	36.80	36.83
Nozzle Pressure Diff.	Pa	236.35	237.08	236.47	236.51	236.60
Atmospheric pressure	kPa	101.031	101.031	101.031	101.031	101.031
Leaving air Specific Volume	m3/kg	0.82	0.82	0.82	0.82	0.82
Air inlet enthalpy	kJ/kg	46.01	46.51	46.33	46.30	46.29
Air outlet enthalpy	kJ/kg	36.48	36.46	36.47	36.49	36.48
Air enthalpy difference	kJ/kg	9.53	10.05	9.86	9.81	9.81
Air mass flow	kg/h	4210.37	4216.95	4211.41	4211.71	4212.61
Air volumetric flow	m3/h	3508.64	3514.12	3509.51	3509.75	3510.51
Fluid volumetric flow	m3/h	3.002	2.999	2.999	2.999	3.000
Fluid side pressure drop	kPa	6.68	6.30	6.16	6.46	6.40
Fluid Density	kg/m3	999.67	999.67	999.68	999.68	999.67
Coarse-adjusting temp.	℃	7.98	8.04	8.03	7.99	8.01
Cond. room unit fluid inlet temp.	℃	7.99	7.98	7.96	7.95	7.97
Cond. room unit fluid outlet temp.	℃	11.50	11.49	11.48	11.49	11.49
Fluid temp difference	℃	3.51	3.50	3.52	3.54	3.52
Average capacity	kW	11.97	11.79	11.92	11.92	11.90
Latent capacity	kW	2.54	3.12	2.90	2.87	2.86
Sensible capacity	kW	8.67	8.73	8.70	8.68	8.69
Air side total capacity	kW	11.21	11.85	11.60	11.54	11.55
Fluid side capacity	kW	12.27	12.24	12.30	12.37	12.30
Thermal balance coefficient	%	8.95	3.31	5.91	6.97	6.28
Air outlet abs. humidity	g/kg	9.32	9.31	9.32	9.32	9.32
Air inlet abs. humidity	g/kg	10.20	10.39	10.32	10.32	10.31
Humidity Ratio Diff.		0.00	0.00	0.00	0.00	0.00

Figure 3.13 : LabVIEW results.

3.3 Measurement Uncertainty Analysis

The uncertainty of the parameters temperature, air flow rate, relative humidity should be taken into account in order to determine the performance of the studies carried out in the experiment and to examine them parametrically. Since these values are taken directly from the measurement results, they can be considered as direct parameters. At the same time, the uncertainties of the parameters derived from them should also be taken into account.

Uncertainty has been calculated using Coblentz method [26] as described in the literature. This method uses a Z parameter directly measured or calculated in the experimental set-up and other variables that influence this Z parameter,

$$w_z = \pm\sqrt{\left(\frac{\partial Z}{\partial z_1}w_1\right)^2 + \left(\frac{\partial Z}{\partial z_2}w_2\right)^2 + \left(\frac{\partial Z}{\partial z_3}w_3\right)^3 \ldots \left(\frac{\partial Z}{\partial z_n}w_n\right)^n} \tag{3.1}$$

The uncertainty calculations of the measuring devices used during the experiment are shown in Table 3.2.

Table 3.2 : Measurement devices uncertainties**.**

Direct Measurement Parameters	Uncertanity Value
Air Temperature –PT100	±0.1°C
Air Relative Humidity	±2 % RH
Termocouple	±1°C
Flowmeter	0.1%
Pressure Difference Sensor	0.1%
Air Volumetric Nozzle	0.3%

The uncertainty calculation is described in detail in Annex A.

3.4 General Test Conditions

This section outlines the structural features of the heat exchanger produced for the tests and the variable parameters on the fluid and air sides in the experiments.

3.4.1 Test sample construction specifications

The fin-and-tube heat exchanger, which was the focus of the thesis, was made of copper tube and aluminium fins. Table 3. shows the structural properties of the tested coil. The S_L and S_T expressions in Table 3 refer to the dimensions in the tube arrangement of the coil. The dimensions represented by S_L and S_T in the coil are illustrated in Figure 3.14. In the coil with 4 rows, the number of tubes in a row is 28. This shows that the total number of tubes in the coil is 112.

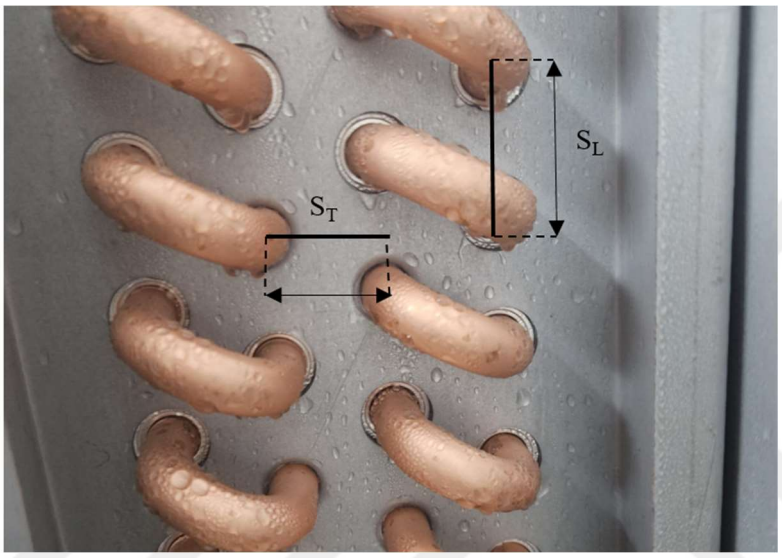

Figure 3.14 : Tube arrangement of test sample.

Table 3.3 : Geometric properties of the test coil.

Parameters	Value
Finned Length	750 mm
Fin Type	Flat
Tube Diameter	12 mm
Tube Thickness	0.32
Fin Thickness	0.12 mm
Tube Material	Copper
Fin Material	Aluminium
S_L	31.75 mm
S_T	28 mm
Tube Count in a Row	28
Row Count	4
Number of Circuits	14

In addition, the finned length expression presented in Table 3.3 is illustrated in Figure 3.15.

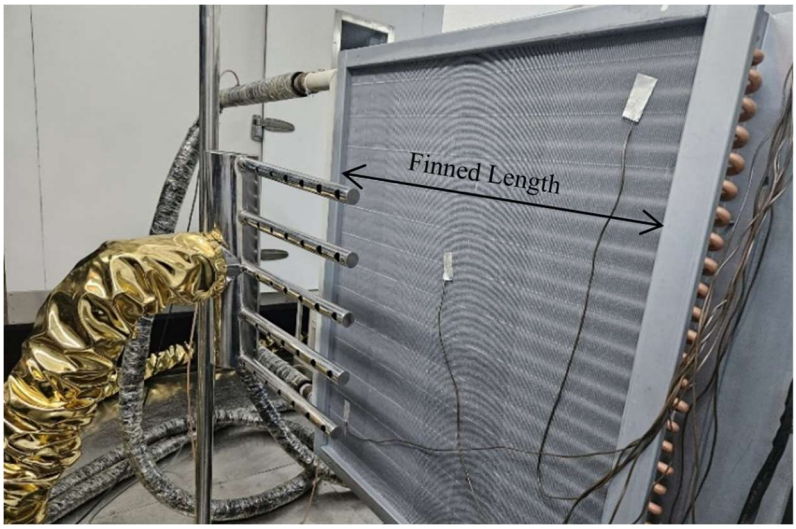

Figure 3.15 : Finned length dimension.

3.4.2 Test sample of air side and water side test conditions

Air inlet temperature was taken as 20 ºC and constant for all test conditions. At the same time, the water side was kept constant at 8 ºC and 3000 kg/h. In this study, there are 5 different air flow rates at each relative humidity value while the studies are carried out at 30%, 70%, 80% and 90% relative humidity. The work carried out within the scope of the thesis was carried out completely for dry and wet conditions. The tests performed at 30% relative humidity represent the coil tests in dry conditions and the tests performed in other conditions represent the wet coil tests. The test conditions are given in Table 3.4 below.

Table 3.4 : Air-side and water side test conditions of the test coil.

Air Inlet Temperature	20 ºC
Inlet Relative Humidity	30-90-80-70
Air Volumetric Flow Rate (m^3/h)	2000-2500-3000-3500-4000
Water Mass Flow Rate (kg/h)	3000
Water Inlet Temperature	8 ºC

3.5 Dry Coil Tests

Section 3.4.2 outlines the test conditions for the dry coil. At a relative humidity of 30%, no condensation is expected within the coil. Given the inlet air temperature and relative humidity value, and the a priori assumption that these values remain constant throughout the dry coil test, the dew point temperature is also known to be constant and equal to 1.89°C throughout the experiment. As the water inlet temperature is 8°C, condensation of water vapour in the air is not possible. The results of the T-type

thermocouple used to control condensation are shown in Table 3. Table 3 shows the experimental results for the dry coil at 5 different air flow rates.

Table 3.5 : Dry conditions test results.

Test Number	Air Volumetric Flow Rate (m^3/h)	Temperature of entrance surface(°C)	Air Temperature(°C)		Water Temperature(°C)		Heat Transfer Capacity (kW)	Air Side Pressure Drop(Pa)
			Inlet Temp. of Air	Out. Temp. of Air	Inlet Temp. of Water	Outlet Temp. of Water		
1	2000	12.4	20	10.3	7.9	9.9	6.8	9.4
2	2500	13.0	20	11.0	8.0	10.3	7.8	12.9
3	3000	13.4	20	11.6	8.0	10.5	8.8	16.8
4	3500	13.7	20	12.0	7.9	10.8	9.6	21.5
5	4000	14.0	20	12.5	8.0	11.0	10.3	26.8

The specific volume of air is calculated by equation 3.2. When the specific volume of air is divided by the air flow rate, the dry air flow rate is obtained as shown in equation 3.3.

$$v_a = \frac{R_a T}{P_a} \tag{3.2}$$

$$\dot{m}_a = \frac{\dot{V}_a}{v_a} \tag{3.3}$$

By obtaining the dry air flow rate, the average specific heat of the air and water vapour mixture and the heat capacity of the coil can be easily calculated with the temperature differences using the formula in Equation 2.2. The heat capacity values calculated in this way are taken directly from the LabVIEW programme and written to the test results.

The air side pressure drops shown in the table are measured using the pressure difference sensors described in the measurement devices section. The air-side pressure drops are in the LabVIEW results.

Figure 3.16 shows the variation of capacity and air-side pressure drop values as a function of air flow rate for the dry coil tests. During the experiment the water flow rate, water and air inlet temperatures were kept constant while the air flow rate was increased. As the air velocity increases, an increase in the heat capacity value and

pressure drop is expected. It can be seen that the results obtained for the dry coil are consistent with this.

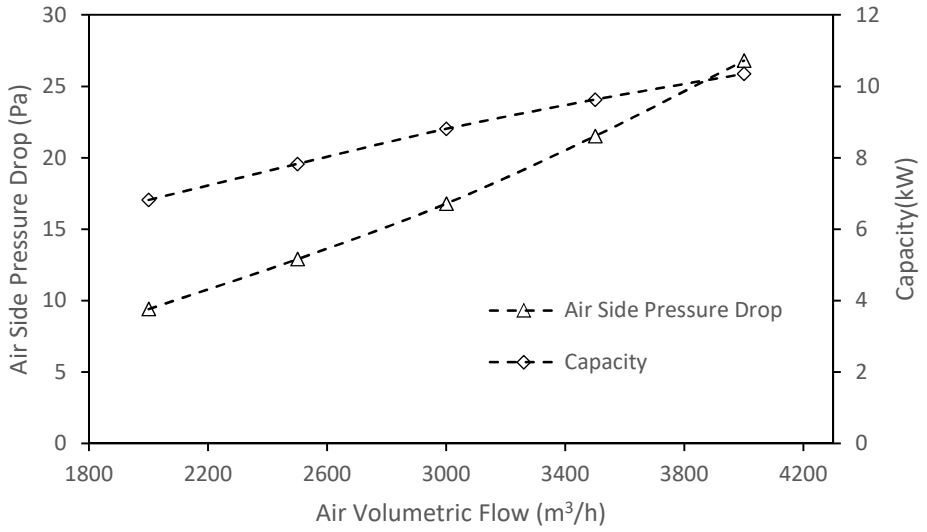

Figure 3.16 : Dry coil heat capacity and air-side pressure loss results.

3.6 Wet Coil Tests

Another part of the study for the thesis is the testing of wet coils. In this thesis, tests were carried out at different relative humidities within the full condensation and partial condensation ranges. The tests at 90%, 80% and 70% relative humidity shown in Table 3. are wet coil tests. The aim of the study is to investigate how the heat transfer coefficient and the air-side pressure drop behave at different relative humidities. Assuming that the air inlet temperature is constant at 20°C, the dew point temperature is change as the relative humidity changes. Since there are 3 different relative humidities in the wet coil test, 3 dew point temperatures can be calculated. According to the results obtained from the psychometric diagram, the dew point temperatures are given in Table 4 below.

Table 3.6 : Dew point temperatures of test conditions.

Ambient Conditions	Dew Point Temperature (ºC)
20 ºC/%70 RH	14.36 ºC
20 ºC/%80 RH	16.44 ºC
20 ºC/%90 RH	18.31 ºC

Table 3.6 shows the results of the tests at 3 different relative humidities and 5 different air flow rates at each relative humidity. According to the value of the inlet surface temperature in these test results, full condensation or partial condensation is interpreted in the coil. Since the inlet surface temperature of the coil at 80% and 90% relative humidity is lower than the dew point of the air, it is expected that the air will condense from the moment it enters the coil. In this case, full condensation is expected at 80% and 90% RH and partial condensation at 70% RH. Figure 3.17 shows the location of one of the 3 thermocouples for the inlet surface temperature value.

Figure 3.17 : Fin inlet zone temperature measurement point.

Equation 2.1 is used to calculate the heat capacity of the coil. The heat capacity is obtained by multiplying the dry air flow rate and the enthalpy differences. The calculation of the dry air flow rate is described in equation 3.2 for dry coil testing. The inlet enthalpy of the air is calculated in the psychometric diagram according to the values in the inlet conditions in Table 3.3 In the psychometric diagram the enthalpy value is plotted according to the inlet air temperature and relative humidity and is taken as the inlet enthalpy for 5 different flow rates at the same relative humidity. Since the temperature and relative humidity kept constant, the inlet enthalpy value do not change even if the air velocity changes. The outlet enthalpy values are taken directly from the LabVIEW programme used for the experimental results. The outlet air enthalpy value can be read from Table 3.7. At the same time, the air-side pressure drops shown in the table are measured using the pressure difference sensor described in the experimental measurement devices section. These values are taken directly from the Labview programme.

Table 3.7 : Wet coil test results.

Air Outlet Entalphy (kj/kg)	Air Volumetric Flow Rate (m^3/h)	Entrance Surface Temp. (°C)	Air Temperature(°C)		Water Temperature(°C)		Heat Transfer Capacity (kW)	Air Side Pressure Drop(Pa)
			Inlet Temp. of Air	Out. Temp. of Air	Inlet Temp. of Water	Out. Temp. of Water		
32.38	2000	14.4	20.1	11.3	8.0	10.8	9.6	9.4
33.94	2500	14.3	20.0	11.9	8.0	11.07	10.6	12.9
35.29	3000	14.3	19.9	12.5	8.0	11.35	11.4	16.8
36.48	3500	14.6	20.0	12.9	8.0	11.49	11.9	21.5
37.6	4000	15.0	20.0	13.4	8.0	11.75	12.4	26.8
33.57	2000	14.8	20.0	11.8	8.0	11.3	11.3	14.7
35.42	2500	14.9	20.0	12.5	8.0	11.7	12.6	20.9
36.84	3000	14.9	20.0	13.1	8.0	11.9	13.4	29.4
38.26	3500	15.4	20.0	13.6	8.0	12.2	14.2	36.1
39.32	4000	15.6	20.0	14.0	8.0	12.5	14.7	45.8
35.04	2000	15.4	19.9	12.3	8.0	11.8	12.9	16.2
37	2500	15.5	20.0	13.1	8.0	12.2	14.2	23.0
38.41	3000	15.4	20.0	13.6	7.9	12.5	15.2	30.3
39.84	3500	15.9	20.0	14.1	8.0	12.7	16	38.1
40.89	4000	16.1	20.0	14.5	8.0	12.9	16.5	47.2

In Figure 3.18, the heat capacity and air-side pressure drop values of the cooling coil experiments performed at 5 different air flow rates and 3 different relative humidities are plotted on the same graph. The results of the experiments performed at 90%, 80% and 70% relative humidity are shown in the graph.

During the experiment, the heat capacity of the coil increases if the other parameters except the air flow rate remain constant and only the air flow rate increases. Figure 3.18 shows that under the same conditions, increasing the relative humidity has a positive effect on the coil capacity. While the heat capacity increases as the relative humidity increases, the air-side pressure drop values are so small that the change in all relative humidities can be neglected. The air-side pressure drop is more significantly influenced by the increase in airflow than by the change in relative humidity.

A conventional method was used to measure the amount of condensation in wet coil tests. The quantity of water condensed in the coil and flowing into a tray in five minutes was calculated. The water in the pan was then poured into a bottle, and the mass of the water condensed in five minutes was calculated and then converted to units of hours. The method by which this is achieved is illustrated in Figure 3.19.

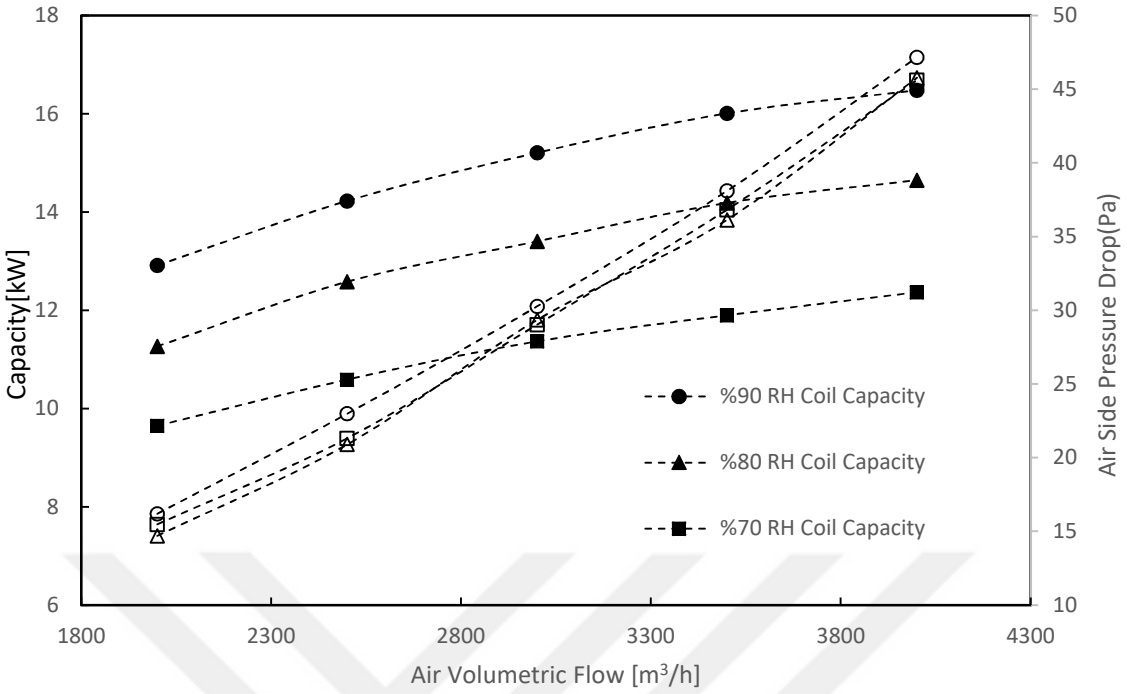

Figure 3.18 : Wet coil capacity and air-side pressure loss results.

Figure 3.19 : Drain tray.

In the experimental studies carried out here, it was observed that the condensation formed at all relative humidities is droplet condensation. Changes in the size and amount of these droplets were observed at different relative humidities and air flow rates. In Figure 3.20, there are visuals to examine the droplet form formed on the fin surface after condensation as a result of the tests performed at different relative humidities. Figure 3.20 represents the test performed at 90% RH and since the condensation is very high, the water droplets of the condensed air are larger and clearer compared to other RHs. Likewise, the condensed water droplets in the tests performed

at 80% RH are larger than the water droplets formed at 70% RH and smaller than the water droplets formed at 90% RH. The least condensation occurred at 70% RH as expected.

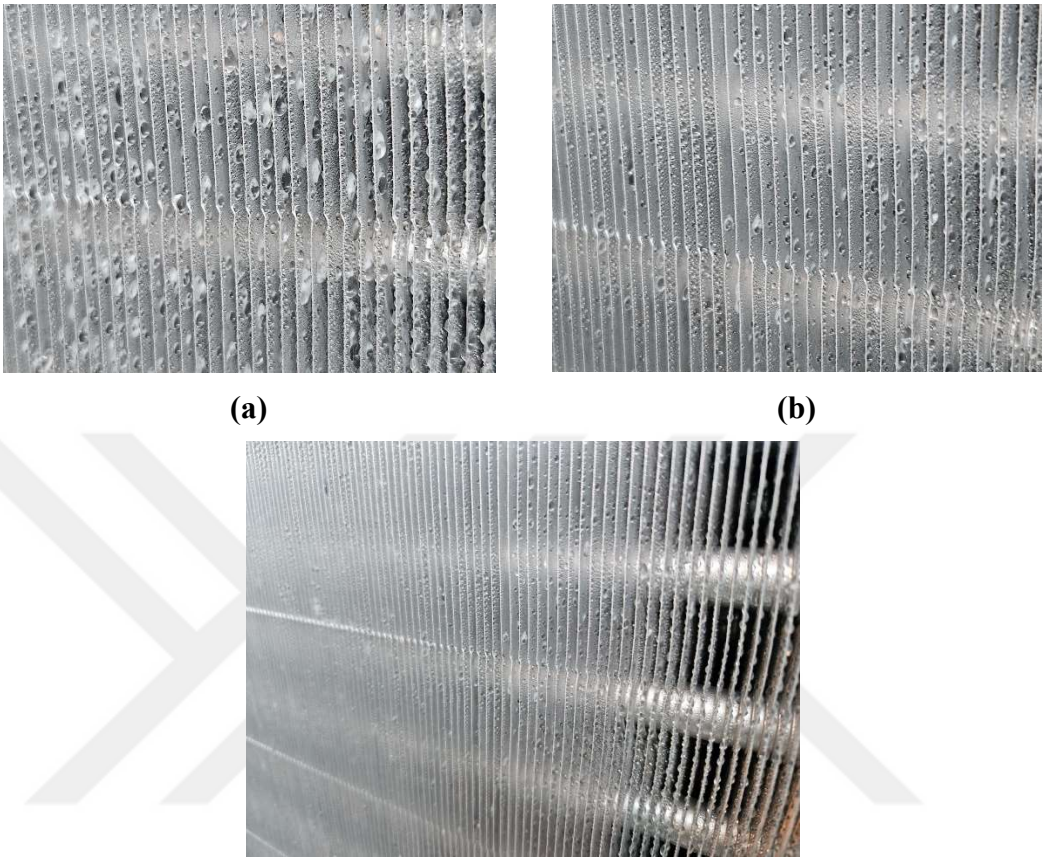

(a) **(b)**

(c)

Figure 3.20 : (a) %90 RH 4000 m^3/h **(b)** %80 RH 4000 m^3/h **(c)** %70 RH 4000 m^3/h.

4. HEAT TRANSFER PERFORMANCE IN DRY AND WET CONDITIONS

This chapter explains how to obtain the heat transfer coefficient and the Colburn j-factor of the heat exchanger. This was tested under dry and wet conditions, using both the experimental results from Chapter 3 and the theoretical analysis from Chapter 2.

4.1 Dry Condition Performance Investigation

The test conditions for dry conditions and the geometrical characteristics of the coil are described in Chapter 3. The performance of this study is analysed by comparing the Colburn J-factor and Reynolds number parameters. To obtain the Colburn factor, the heat transfer coefficient, which is a dimensional parameter, was obtained for the air side and the fluid side. For the performance analysis of dry conditions, the total heat transfer equation 2.3 given in Chapter 2 is used.

U_0 total heat transfer coefficient represents the total heat transfer equation. A_0, total external surface area is represented by. The total surface area was calculated in accordance with the surface area formula defined in equations 2.1 to 2.7. The total surface area of the tested coil is 55.04 m². F expression in this context represents the logarithmic temperature correction factor. Given that the heat transfer in four or more rows of coils can be characterised as cross flow, the F factor is found to be very close to 1. Consequently, it is considered to be constant at 1.

Q expression was then taken as the average capacity in the experimental results. The average capacity expression in the experimental results is the average of the fluid-side capacity and air-side capacity obtained in the experimental outputs. Furthermore, ΔT_{lm} is also derived from the experimental results in order to examine the total heat transfer performance. The logarithmic mean temperature expression is defined and explained in Chapter 2. If the U_0 obtained from the experimental results are substituted in the equation to examine the total heat transfer performance, it should be noted that certain assumptions have been made in the studies carried out to obtain it.

1. It is assumed that the coil surface and air are free from contamination and that the effects of fouling factor are not considered.

2. It is assumed that the system is stead-state and mathematical equations reduced in accordance it.

3. The contact resistance between the tube and the fin inside the coil is not considered.

4. It is assumed that the heat transfer coefficient inside the tube is constant.

5. It is assumed that the heat conduction coefficients of the tube and fin materials remain constant and invariant with temperature.

6. It is assumed that radiation transfer of heat is negligible.

7. While the calculations are based on the geometric properties of the coil, it should be noted that tolerances in the manufacturing parameters are not taken into account.

The total heat transfer coefficient is obtained using Equations 2.21 and 2.12, as presented in Chapter 2. The Gnielinski correlation is presented in these equations. The Reynolds number required for the Nusselt correlation is calculated. The internal tube diameter is taken as the characteristic length.

$$\mathrm{Re} = \frac{\rho V D_i}{\mu} \tag{4.1}$$

Among the expressions in the Gnielinski correlation, the Reynolds number is dependent upon the velocity and tube diameter, as well as the thermophysical properties of the fluid. In order to maintain consistency, the diameter of the tube through which the fluid passes and the water flow rate in each experiment were held constant. Given that the water flow rate and velocity were maintained throughout the experiments, the Reynolds number was found to be constant, with a value of Re = 5425. It was also assumed that the inlet water temperature remained constant at 8°C throughout the experiments. The temperature of the water exiting the tube is dependent on the capacity of the tube. However, the impact of this temperature change on the thermophysical properties is not considered, and the heat transfer coefficient in the tube is assumed to be the same for all experiments, with the Reynolds number and Prandtl number held constant in the tube.

Once the heat transfer coefficient in the tube has been determined in accordance with Equation 2.25, the remaining unknown parameters are the air-side heat transfer coefficient and surface efficiency. The parameter that indicates the thermal performance of a fin in the coil is the fin efficiency. The expression that demonstrates the performance of that surface over a fin array is the surface efficiency. A detailed explanation of the surface efficiency and fin efficiency expressions can be found in Chapter 2.

The heat transfer coefficient of the air-side is required to obtain the surface efficiency (η_0). Therefore an iterative solution is performed. The equation in 2.34 is used to calculate the surface efficiency. A_f is the fin surface area, while A_0 is the total surface area. η_f is represent the fin efficiency. To calculate the surface efficiency, it is necessary to know the fin efficiency as seen the equation 2.34. Therefore, the fin efficiency and the heat transfer coefficient are not independent. The fin efficiency is calculated according to equation 2.31. The *X* expression is in Equation 2.32. Since the fin efficiency depends on many parameters such as heat transfer coefficient, heat conduction coefficient, equivalent diameter, it is combined in a single expression.

The heat transfer coefficient expression in the fin efficiency equation is written explicitly and when integrated into the equation, it is transformed into an simple equation as 4.2. By iteratively solving the equation, the air-side heat transfer coefficient, fin efficiency and surface efficiency were found.

$$\eta_f = \frac{\tanh(\varphi \frac{D_o}{2} \sqrt{\frac{2h_o}{k_{tube}\delta}})}{\varphi \frac{D_o}{2} \sqrt{\frac{2h_o}{k_{tube}\delta}}} \tag{4.2}$$

For dry conditions, there are 5 different Reynolds numbers because it is carried out at 5 different air flow rates. Figure 4.1 shows the fin efficiency -Reynolds number plotted at 5 different Reynolds numbers. As the Reynolds number on the air-side increases, the efficiency of the fin decreases.

In the comparison of Reynolds Numbers shown in the results graphs, the average air temperature was used as the air temperature to calculate the thermophysical properties. To find the Reynolds number of the air side, the velocity at the smallest cross section

is taken as the reference. The tube outside diameter was used as the characteristic length in the Reynolds number formula. [13]

$$V_{air\max} = \frac{V_{air}}{A_{\min}} \tag{4.3}$$

$$\mathrm{Re} = \frac{\rho_{air} V_{air\max} D_0}{\mu_{air}} \tag{4.4}$$

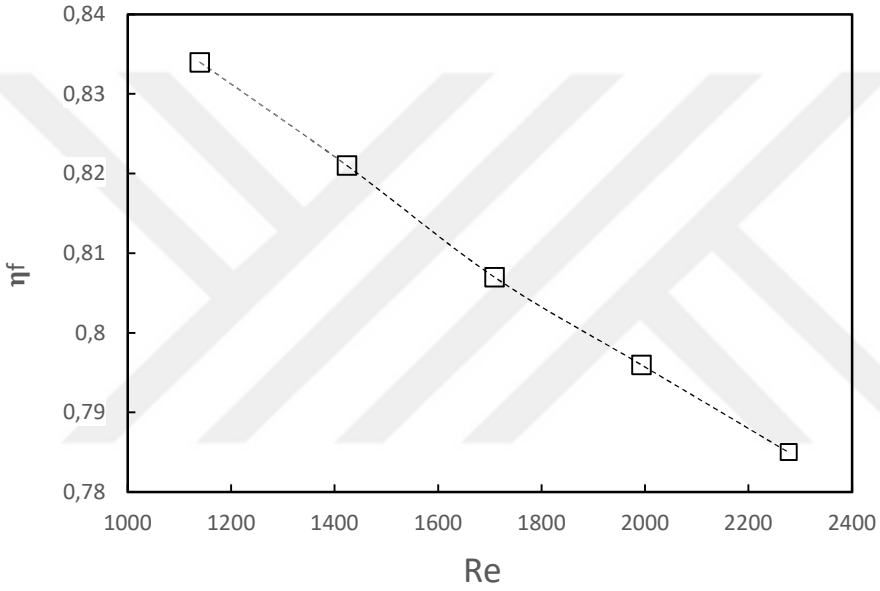

Figure 4.1 : Re-η_f graph under dry conditions.

Once the air side heat transfer coefficient and surface area efficiency values have been determined, the Colburn j-factor can be defined. The heat transfer coefficient and pressure drop performance of heat exchangers have been reported with the Colburn j-factor at different Reynolds numbers. The Colburn j-factor is calculated from Equation 4.5.

$$j = St\,\mathrm{Pr}^{2/3} \tag{4.5}$$

The Stanton expression in Equation 4.5 is a dimensionless expression that gives the ratio of the heat transferred to a fluid to the heat capacity of the fluid. It also gives information about the thermal performance of a physical state with known flow

dynamics. The Stanton number, which is a dimensionless expression, is given in Equation 4.6.

$$St = \frac{Nu}{\mathrm{Re}\,\mathrm{Pr}} \tag{4.6}$$

If it is desired to write the heat transfer coefficient as a function of the Colburn j-factor and the expressions are expanded in the St number;

$$j = \frac{Nu}{\mathrm{Re}\,\mathrm{Pr}^{1/3}} \qquad j = \frac{h_o}{G_a \dfrac{Cp_a}{\mathrm{Pr}_a^{2/3}}} \tag{4.7}$$

It is written as Equation 4.7. To analyse the thermal performance in dry conditions, the Colburn j-factor - Reynolds number plot in Figure 4.2 can be examined.

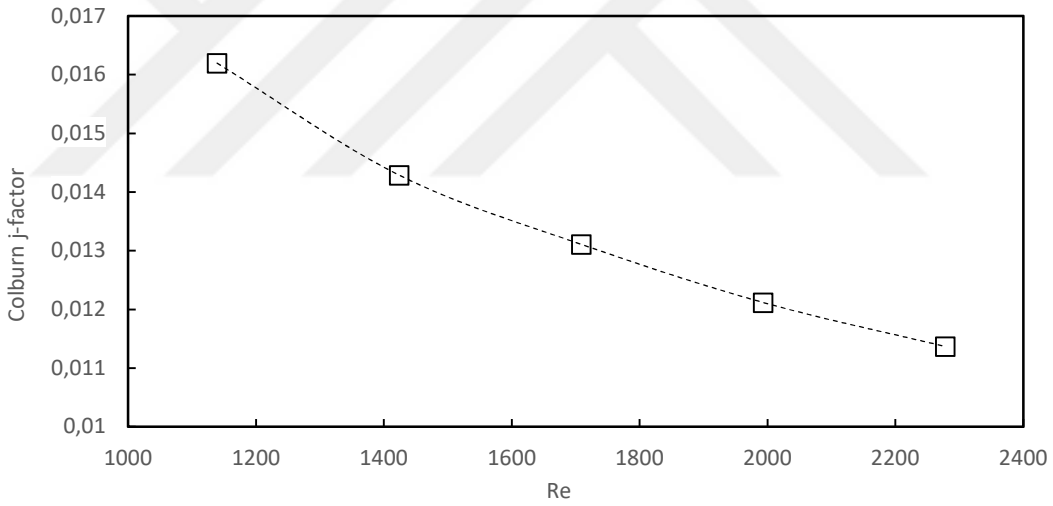

Figure 4.2 : Re- colburn j-factor graph in dry conditions.

Studies similar to the experimental study are also available in the literature. Therefore, this experimental study has been compared with the correlations mentioned in chapter 1. The graph in Figure 4.3 compares the Colburn j-factor obtained from the experimental results with the correlation in Rich, D. (1973), which is the only study in the literature with a geometry of 31.75 mm x 28 mm, and the correlation in VDI Heat Atlas. (2011), which is one of the reference books for the calculation of fin-and-tube heat exchangers. (Air Side R.LWebb) In equations 4.8 and 4.9, the correlation utilised

by Rich is presented. The equations presented in Equations 2.26 and 2.27, as detailed in Chapter 1, are employed in the VDI Heat Atlas.

$$J_{4,Rich} = 0.195\mathrm{Re}_{air}^{-0.35} \tag{4.8}$$

$$h_{Rich} = \frac{J_4 G_a C_{p,a}}{\mathrm{Pr}_a} \tag{4.9}$$

These comparisons have also been analysed for 5 different Reynolds Numbers. The hydraulic diameter in the reference Reynolds number calculation is the tube diameter in all correlations. In Figure 4.4 this has been done with a similar heat transfer coefficient.

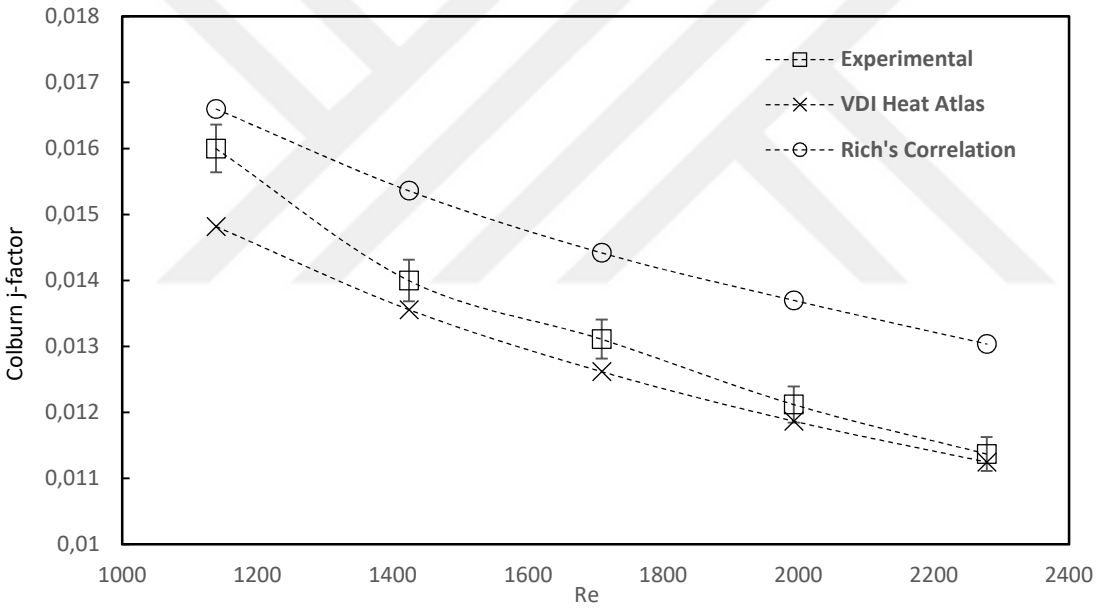

Figure 4.3 : Colburn J-factor and Reynolds number graph obtained from correlations with experimental study.

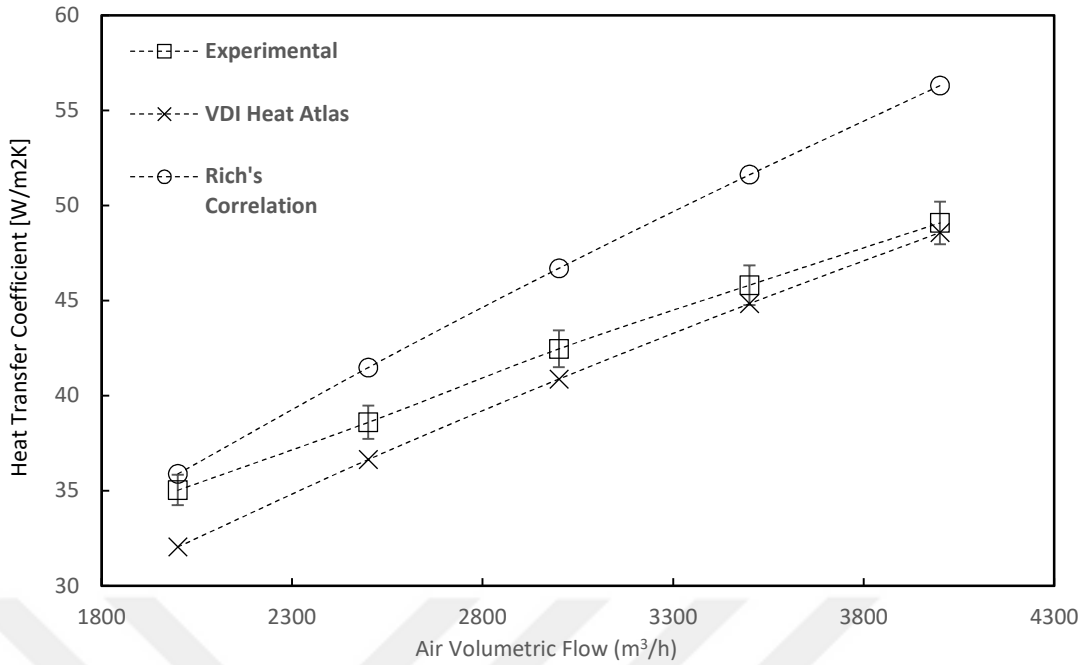

Figure 4.4 : Heat transfer coefficient and Reynolds number graph obtained from correlations with experimental study.

4.2 Wet Conditions Performance Investigation

The test conditions and geometric characteristics of the coil given in section 3 for dry conditions are also valid for the experimental work to be carried out in wet conditions. There are common points in the theoretical analysis calculations of the wet and dry experimental studies. The Colburn J-factor and Reynolds number have been compared to examine the performance of the wet tests. The Threlkeld method was used to obtain the Colburn J-factor. The Threlkeld method was used to obtain the air-side heat transfer coefficient, which is a dimensional parameter, and then to calculate the Colburn J-factor. The Threlkeld method is based on the logarithmic enthalpy difference in equation 2.35.

The value $U_{0,w}$ in the total heat transfer equation is the total heat transfer coefficient for the wet condition. The surface area of the coil is the same in wet and dry conditions. The calculation to be made using the Threlkeld method is similar to the basic heat transfer calculation. The capacity value taken from the experiment is used as the heat capacity value. The expression Q in equation 2.35 represents the wet capacity, which is the sum of the latent and sensible heat in the experimental data.

Δi_m is the logarithmic enthalpy difference obtained from the experimental results, just like the logarithmic temperature difference, to examine the overall heat transfer performance. The logarithmic enthalpy difference Δi_m is explained in detail in equation 2.34.

Substituting the data obtained from the experimental results into the equation given to study the total heat transfer performance, $U_{0,w}$ is obtained. Some assumptions have been made in the studies carried out to obtain $U_{0,w}$.

1. It is assumed that the coil surface and air are free from contamination and that the effects of fouling factor are not considered.

2. It is assumed that the system is stead-state and mathematical equations reduced in accordance it.

3. The contact resistance between the tube and the fin inside the coil is not considered.

4. It is assumed that the heat transfer coefficient inside the tube is constant.

5. It is assumed that the heat conduction coefficients of the tube and fin materials remain constant and invariant with temperature.

6. It is assumed that radiation transfer of heat is negligible.

7. While the calculations are based on the geometric properties of the coil, it should be noted that tolerances in the manufacturing parameters are not taken into account.

8. The correction factor F is assumed to be '1' since it is very close to one [25].

To switch from the total heat transfer coefficient to the air-side heat transfer coefficient, the parameters must be found in Equation 4.10.

$$\frac{1}{U_{0,w}A_0}=\frac{1}{R_t}=\frac{b'_r}{h_iA_i}+\frac{b'_p\ln(\frac{D_o}{D_i})}{2\pi k_{tube}L}+\frac{1}{h_{o,w}\left[\frac{A_{p,o}}{b'_{wf,p,out}}+\frac{A_f\,\eta_{f,wet}}{b'_{wf}}\right]} \tag{4.10}$$

The values b'_r, b'_p, $b'_{wf,p,out}$, b'_{wf} which are parameters that never seen in the calculations in dry conditions, actually represent specific heats. The reason they are shown with different indices is that the enthalpy of saturated humid air is the ratio of

different temperatures. These different temperatures include the tube outer surface temperature and the average fin surface temperature.

The tube outer surface temperature and the average fin surface temperature are calculated using the basic heat transfer calculations given in chapter 2. To obtain the b'_r, b'_p, $b'_{wf,p,out}$ b'_{wf} values, the average fin surface temperature and the outer tube surface temperature must be calculated. b'_r, b'_p, $b'_{wf,p,out}$ b'_{wf} calculations are given in Equation 4.12, 4.13 and 4.14 [25].

$$b'_r = \frac{\left(i_{r,p,in,m} - i_{r,m}\right)}{\left(T_{r,p,in,m} - T_{r,m}\right)}, b'_p = \frac{\left(i_{r,p,out,m} - i_{r,p,in,m}\right)}{\left(T_{r,p,out,m} - T_{r,p,in,m}\right)} \tag{4.12}$$

$$b'_{wf,p,out} = \frac{H_{humidair}(T_{o,s}+1,1) - H_{humidair}(T_{o,s}-1,1)}{\left(T_{o,s}+1-T_{o,s}-1\right)} \tag{4.13}$$

$$b'_{wf,f} = \frac{H_{humidair}(T_{s}+1,1) - H_{humidair}(T_{s}-1,1)}{\left(T_{s}+1-T_{s}-1\right)} \tag{4.14}$$

The values of $T_{o,s}$ and T_s used in Equation 4.13 and 4.14 are given in Equations 4.15 and 4.16 for the calculation of the tube outer surface temperature and the average fin surface temperature, respectively.

$$T_{water,average} = \frac{T_{f,i} + T_{f,o}}{2} \tag{4.15}$$

$$T_{o,s} = \Delta T + T_{water,average}\ ,\ \ \Delta T = T_{o,s} - T_{water,average} \tag{4.16}$$

The thermal resistance of the tube metal in equation 4.17 and the internal convection resistance of the fluid in the tube have been used in the calculations. As the change in water temperature is very small, the average water temperature is taken as the correct value.

$$R_{total} = \frac{1}{h_i A_i} + \frac{\ln(\frac{D_o}{D_i})}{2\pi k_{tube} L} \tag{4.17}$$

Fin efficiency is used to determine the average fin surface temperature. Fin efficiency is defined as the ratio of the heat dissipated by the fin to the maximum heat that can be dissipated by the fin under these conditions. Since the heat transfer coefficient and surface area are the same for both, the temperature difference determines the ratio. The heat dissipated from the fin is the temperature difference between the average fin surface temperature and the air temperature. The maximum heat dissipated is the difference between the temperature at the bottom of the fin, i.e. the temperature considered to be the outer surface of the tube, and the air temperature. The ratio of these two temperature differences is also the efficiency of the fin [9].

$$\eta_{f,wet} = \frac{T_s - T_a}{T_{o,s} - T_a} \tag{4.18}$$

Since the fin efficiency is a parameter that depends on the heat transfer coefficient, the result is obtained by simultaneous solution. Since the water flow rate is kept constant in the fin-and-tube heat exchanger experiments carried out under wet conditions. The definitions of the unknowns given in equation 4.10 are used, except for the term $h_{o,w}$ All parameters are related to each other to obtain the $h_{o,w}$ expression. Therefore, when all equations are converted to the unknown $h_{o,w}$ they are converted to an equation with one unknown and solved. The method of calculating the Colburn j-factor is the same as for dry conditions. The Colburn j-factor is obtained by using the air side heat transfer coefficient value calculated for the wet coil using equations 4.3 and 4.4.

The graphs below show the results of the wet tests at 90%, 80% and 70% respectively. Figure 4.5 shows the variation of the heat transfer coefficients at three different relative humidities as a function of Reynolds number. Figure 4.6 shows the variation of the Colburn J-factor with respect to the Reynolds number in the tests where heat transfer coefficients were obtained.

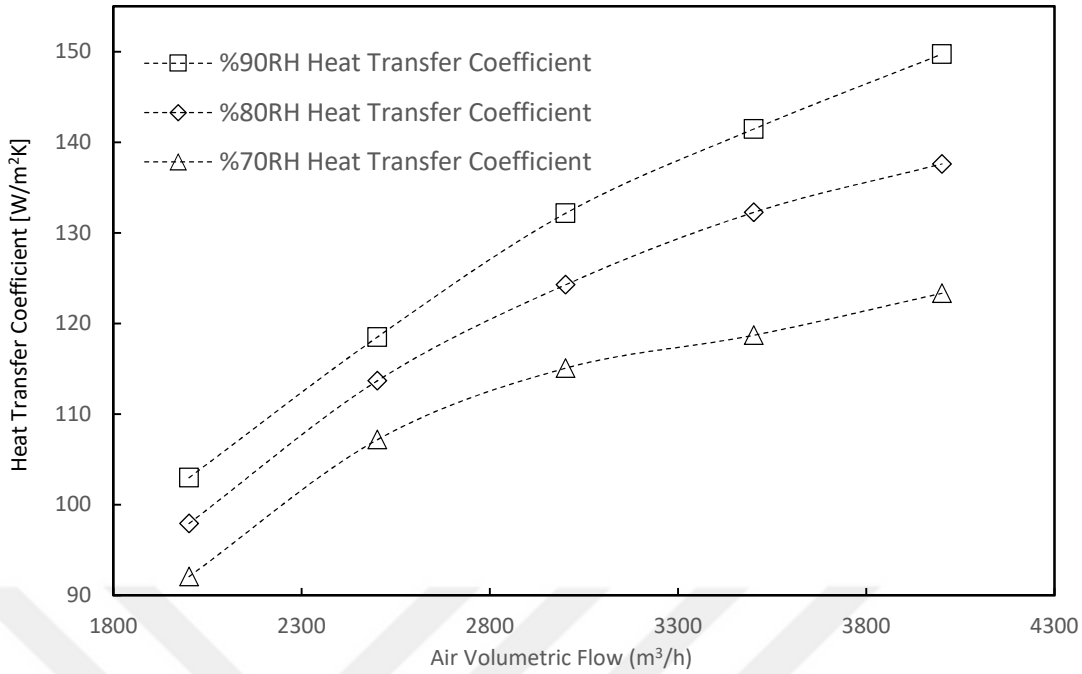

Figure 4.5 : Air volumetric flow-heat transfer coefficient graph in wet conditions.

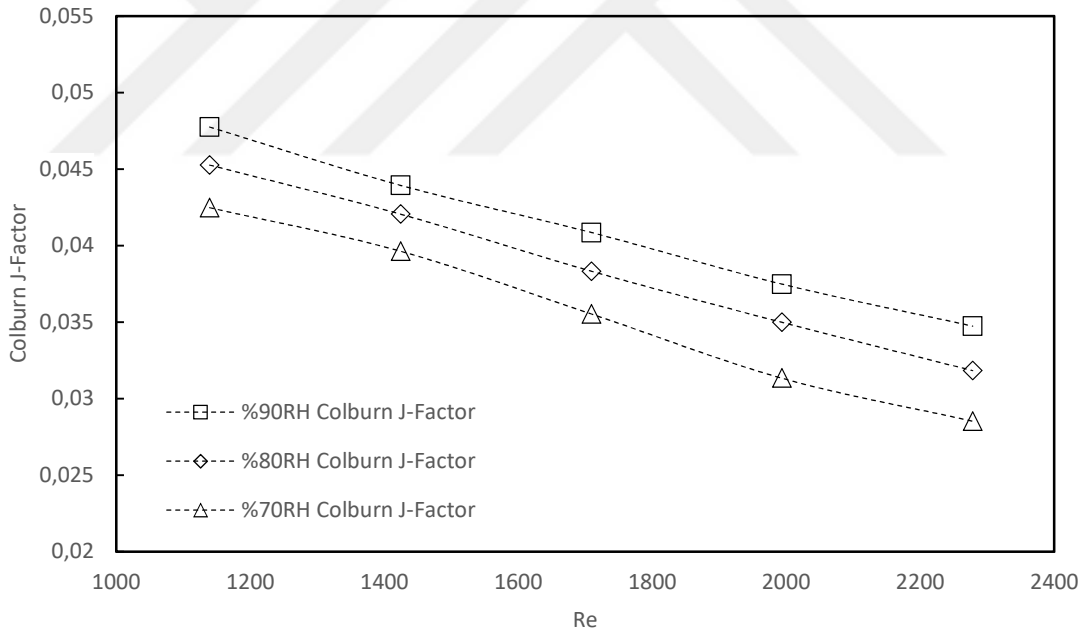

Figure 4.6 : Reynolds number-colburn j-factor graph in wet conditions.

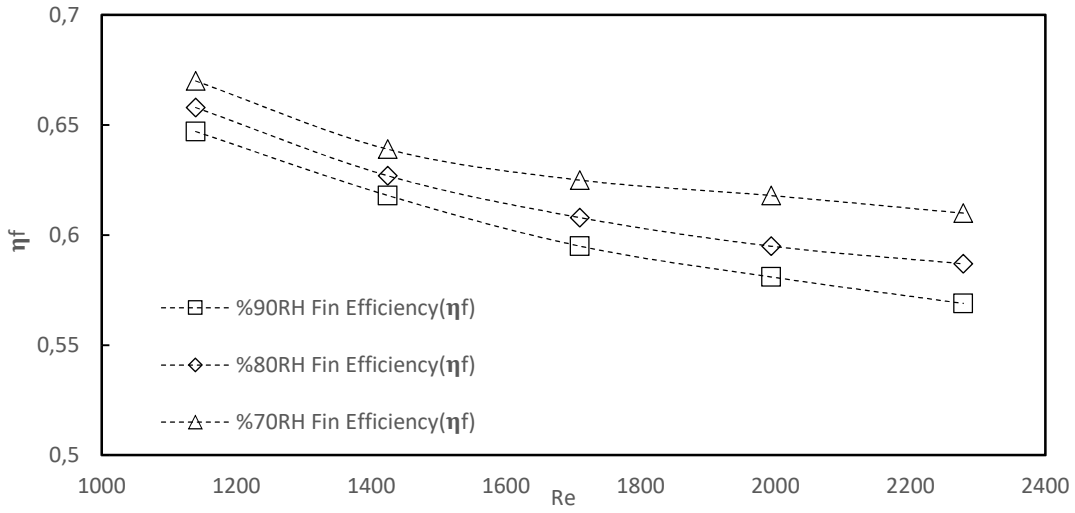

Figure 4.7 : Fin efficiency (η) and Reynolds number graph in wet conditions.

Given the absence of a study in the literature with a geometry comparable to that of the tube arrangement of the experimental study conducted within the scope of this thesis, it was not possible to establish any correlation.

5. CONCLUSION

This study was considered a fin-and-tube heat exchanger with a four row and 31.75 x 28 mm tube arrangement at different relative humidities. The experimental studies were carried out for dry conditions without condensation and for wet conditions with condensation. For dry conditions, comparisons were made with other correlations in the literature. Given the lack of suitable geometry for wet conditions in the literature, no comparison could be made with the existing correlations. We have obtained results regarding the thermal performance of the fin-and-tube heat exchanger. These results are discussed in terms of air-side pressure loss, heat transfer coefficient and Colburn j-factor.

- In dry conditions, as the air velocity increases, the thermal capacity and air-side pressure loss value increase. When the air velocity is doubled, the air side pressure loss value increases by 2.85 times.
- In dry conditions, the fin efficiency decreases as the Reynolds number increases. When the Reynolds number is doubled, the fin efficiency decreases by 6.2%.
- The results of the humid and dry air tests demonstrate that the Colburn j-factor decreases when the Reynolds number is increased. In contrast, the heat transfer coefficient forms a completely opposite behaviour. As the Reynolds number increases, the heat transfer coefficient also increases. When the Reynolds number is doubled, the Colburn j-factor decreases by 30.5% while the heat transfer coefficient value increases by 35.5%.
- The dry air test results clearly show that the heat transfer coefficient and Colburn j-factor values obtained from the experimental results are most similar to the correlation in the VDI Heat Atlas in the literature. There was a 10% difference at low Reynolds numbers, but this decreased to 1% when the Reynolds number increased. In the Rich[2] correlation, the results were quite similar at low Reynolds numbers, but when the Reynolds number increased, the results diverged from the results.

- It should be noted that the tube arrangements used in the fin-and-tube heat exchangers in the studies of Wang et al. and McQuiston differ from the tube arrangement of the test coil used in this thesis. As a result, a direct comparison is not possible.
- In wet conditions, Colburn j-factor and heat transfer coefficient increased as the relative humidity increased. At the same Reynolds number and different relative humidities in wet conditions, the results vary between 3% and 10%.
- When the air side pressure loss values of dry and wet conditions are compared at the same Reynolds number, there is an average of 71% difference with a minimum of 56% and a maximum of 80% difference.
- Heat transfer coefficient and Colburn j-factor values are compatible with each other. While the heat transfer coefficient value in wet and dry conditions is approximately 2.5 times higher at low relative humidity, this ratio increases up to 3.1 times at %90 relative humidity.

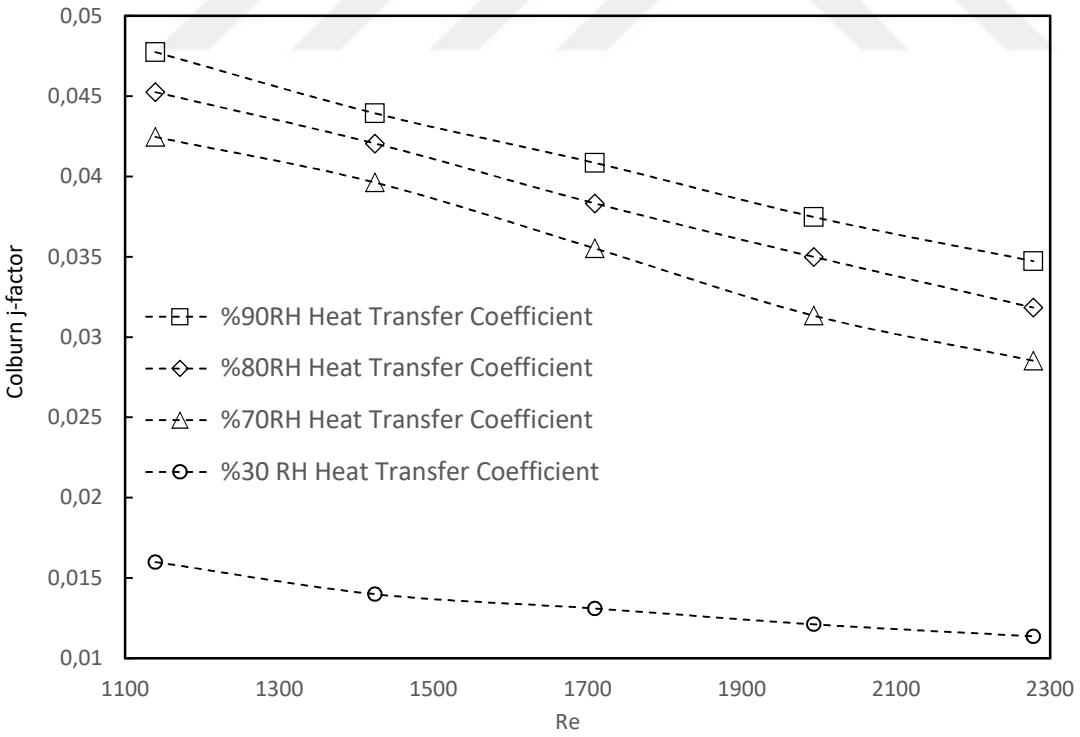

Figure 5.1 : The graph of the colburn j-factor and Reynolds number.

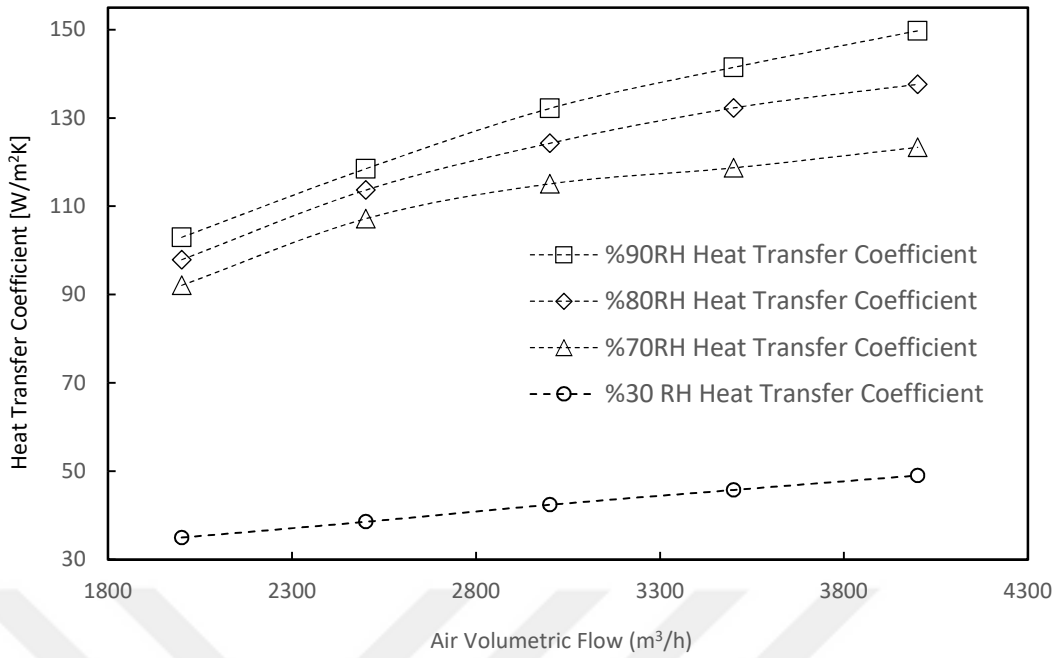

Figure 5.2 : The graph of the heat transfer coefficient and air volumetric flow.

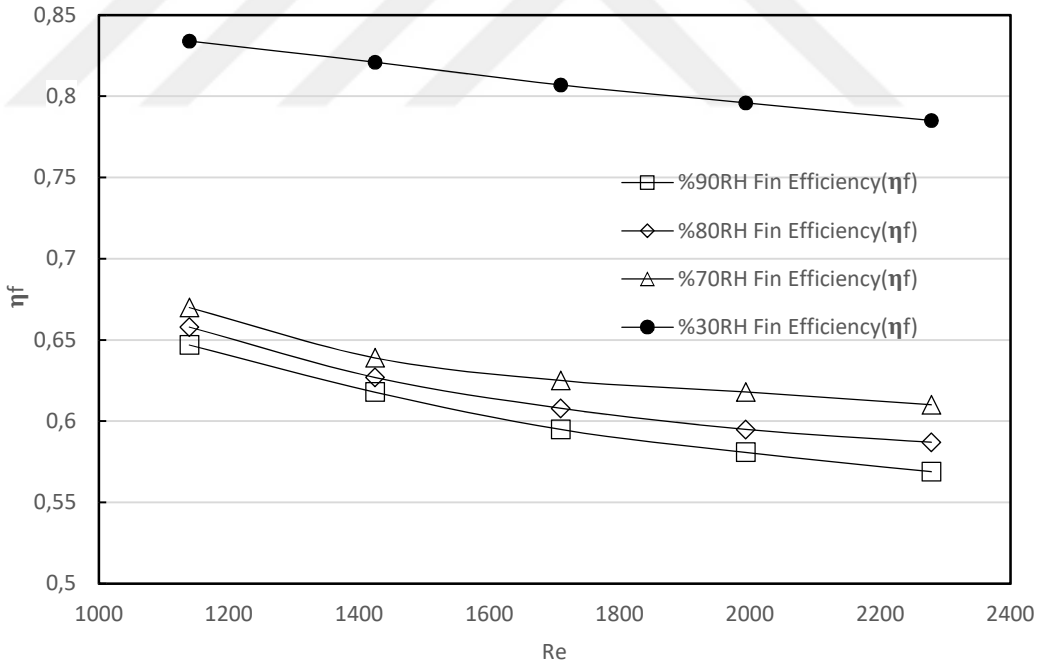

Figure 5.3: The graph of the fin efficiency and Reynolds number.

REFERENCES

[1] Wang, C. C., & Liaw, J. S. (2012). Air-side performance of herringbone wavy fin-and-tube heat exchangers under dehumidifying condition - Data with larger diameter tube. *International Journal of Heat and Mass Transfer*, *55*(11–12), 3054–3060. https://doi.org/10.1016/j.ijheatmasstransfer.2012.02.025

[2] Kim, N. H., & Kim, S. H. (2010). Dry and wet air-side performance of a louver-finned heat exchanger having flat tubes. *Journal of Mechanical Science and Technology*, *24*(7), 1553–1561. https://doi.org/10.1007/s12206-010-0409-1

[3] Ma, X., Ding, G., Zhang, Y., & Wang, K. (2009). Airside characteristics of heat, mass transfer and pressure drop for heat exchangers of tube-in hydrophilic coating wavy fin under dehumidifying conditions. *International Journal of Heat and Mass Transfer*, *52*(19–20), 4358–4370. https://doi.org/10.1016/j.ijheatmasstransfer.2009.03.066

[4] Kuvannarat, T., Wang, C. C., & Wongwises, S. (2006). Effect of fin thickness on the air-side performance of wavy fin-and-tube heat exchangers under dehumidifying conditions. *International Journal of Heat and Mass Transfer*, *49*(15–16), 2587–2596. https://doi.org/10.1016/j.ijheatmasstransfer.2006.01.020

[5] Wang, C. C., Hsieh, Y. C., & Lin, Y. T. (1997). Performance of plate finned tube heat exchangers under dehumidifying conditions. *Journal of Heat Transfer*, *119*(1), 109–117. https://doi.org/10.1115/1.2824075

[6] Hu, W. L., Ma, A. J., Guan, Y., Cui, Z. J., Zhang, Y. B., & Wang, J. (2021). Experimental study of the air side performance of fin-and-tube heat exchanger with different fin material in dehumidifying conditions. *Energies*, *14*(21). https://doi.org/10.3390/en14217030

[7] Kayansayan, N. (1993). Heat transfer characterization of flat plain fins and round tube heat exchangers. *Experimental Thermal and Fluid Science*, *6*(3), 263–272. https://doi.org/10.1016/0894-1777(93)90067-S

[8] Yan, W. M., & Sheen, P. J. (2000). Heat transfer and friction characteristics of fin-and-tube heat exchangers. *International Journal of Heat and Mass Transfer*, *43*(9), 1651–1659. https://doi.org/10.1016/S0017-9310(99)00229-X

[9] Incropera, F. P., and Dewitt, D. P. (1985). Fundamentals of Heat and Mass Transfer, 2nd ed., Wiley, New York, pp. 309-404.

[10] Wang, C. C., Lin, Y. T., & Lee, C. J. (2000). An airside correlation for plain fin-and-tube heat exchangers in wet conditions. *International Journal of Heat and Mass Transfer*, *43*(10), 1869–1872. https://doi.org/10.1016/S0017-9310(99)00240-9

[11] Liu, Y. C., Wongwises, S., Chang, W. J., & Wang, C. C. (2010). Airside performance of fin-and-tube heat exchangers in dehumidifying conditions - Data with larger diameter. *International Journal of Heat and Mass Transfer*, *53*(7–8), 1603–1608. https://doi.org/10.1016/j.ijheatmasstransfer.2009.12.015

[12] McQuiston, F. C. (1980). *Finned tube heat exchangers: state of the art for the air side.*

[13] ***VDI Heat Atlas*****. (2010)**. Springer Berlin Heidelberg. https://doi.org/10.1007/978-3-540-77877-6

[14] Kays, W. M., & London, A. L. (1984). *Compact heat exchangers. Third Edition.*

[15] Wang, C. C., Lee, W. S., Sheu, W. J., & Chang, Y. J. (2002). A comparison of the airside performance of the fin-and-tube heat exchangers in wet conditions; With and without hydrophilic coating. *Applied Thermal Engineering*, *22*(3), 267–278. https://doi.org/10.1016/S1359-4311(01)00090-4

[16] Gray, D. L., & Webb, R. L. (1986). Heat Transfer And Friction Correlations For Plate Finned-Tube Heat Exchangers Having Plain Fins. *Proceeding of International Heat Transfer Conference 8*, 2745–2750. https://doi.org/10.1615/IHTC8.1200

[17] Halıcı, F., Taymaz, İ., & Gündüz, M. (2001). The effect of the number of tube rows on heat, mass and momentum transfer in flat-plate finned tube heat exchangers. *Energy*, *26*(11), 963–972. https://doi.org/10.1016/S0360-5442(01)00048-2

[18] Rich, D. G.(1975). The Effect of the Number of Tube Rows on Heat Transfer Performance of Smooth Plate Fin-and-Tube Heat Exchangers, *ASHRAE* Trans., 81(1), 307-317.

[19] Korte, C., & Jacobi, A. M. (2001). Condensate Retention Effects on the Performance of Plain-Fin-and-Tube Heat Exchangers: Retention Data and Modeling. *Journal of Heat Transfer*, *123*(5), 926–936. https://doi.org/10.1115/1.1391276

[20] Gnielinski, V. (2013). On heat transfer in tubes. *International Journal of Heat and Mass Transfer*, *63*, 134–140. https://doi.org/10.1016/j.ijheatmasstransfer.2013.04.015

[21] J.L. Threlkeld. (1970). Thermal Environmental Engineering, Prentice-Hall, New York.

[22] R.J. Myers. (1967). The effect of dehumidification on the air-side heat transfer coefficient for a finned-tube coil, MS Thesis, University of Minnesota, Minneapolis.

[23] Bump, T. R. (1963). Average Temperatures in Simple Heat Exchangers. *Journal of Heat Transfer*, *85*(2), 182–183. https://doi.org/10.1115/1.3686051

[24] Rich, D. G.(1973). The Effect of Fin Spacing on the Itcat Transfer and Friction Performance of Multi-row, Smooth Plate Fin-and-Tube Heat Exchangers, *ASHRAE* Trans., 79(2), 137 145.

[25] Pirompugd, W., Wang, C.-C., & Wongwises, S. (2007). A Fully Wet and Fully Dry Tiny Circular Fin Method for Heat and Mass Transfer Characteristics for Plain Fin-and-Tube Heat Exchangers Under Dehumidifying Conditions. *Journal of Heat Transfer*, *129*(9), 1256–1267. https://doi.org/10.1115/1.2739589

[26] Coblentz LC. (2009). Uncertainty Analysis of Heat Exchanger. Msc Thesis, Mechanical Engineering in the Faculty of Engineering at the Rand Africaans University, Johannesburg, South Africa.

APPENDICES

APPENDIX A: Uncertanity Calculation Method

APPENDIX A

Fluid Side Capacity Uncertanity Calculation

$$Q = \dot{m}_w C_{p,w}(T_{f,o} - T_{f,i}) \quad = \quad \rho_f V_f C_{p,f}(T_{f,o} - T_{f,i})$$

$$Q = Q(\rho_f, V_f, C_{p,w}, T_{f,o}, T_{f,i}$$

$$\delta Q = \sqrt{\left(\frac{\partial Q}{\partial \rho_f} w_{\rho,w}\right)^2 + \left(\frac{\partial Q}{\partial V_f} w_{\dot{V}}\right)^2 + \left(\frac{\partial Q}{\partial Cp_f} w_{Cp_f}\right)^2 + \left(\frac{\partial Q}{\partial (T_{f,o} - T_{f,i})} w_{(T_{f,o}-T_{f,i})}\right)^2 + \left(-\frac{\partial Q}{\partial (T_{f,o} - T_{f,i})} w_{(T_{f,o}-T_{f,i})}\right)^2}$$

Air Side Capacity Uncertanity Calculation

$$Q = \dot{m}_a C_{p,a}(T_{a,o} - T_{a,i}) \quad = \quad \rho_a V_a C_{p,a}(T_{a,o} - T_{a,i})$$

$$Q = Q(\rho_a, V_a, C_{p,a}, T_{a,o}, T_{a,i}$$

$$\delta Q = \sqrt{\left(\frac{\partial Q}{\partial \rho_a} w_{\rho,a}\right)^2 + \left(\frac{\partial Q}{\partial V_a} w_{\dot{V},a}\right)^2 + \left(\frac{\partial Q}{\partial Cp_a} w_{Cp_a}\right)^2 + \left(\frac{\partial Q}{\partial (T_{a,o} - T_{a,i})} w_{(T_{a,o}-T_{a,i})}\right)^2 + \left(\frac{\partial Q}{\partial (T_{a,o} - T_{a,i})} w_{(T_{a,o}-T_{a,i})}\right)^2}$$

Fluid Side Capacity Uncertanity Calculation

$$\mathrm{Re} = \frac{V_f D_i}{\nu_f}$$

$$\mathrm{Re} = \mathrm{Re}(V_f D_i, \nu_f)$$

$$\mathrm{Re} = \sqrt{\left(\frac{\partial \mathrm{Re}}{\partial V_f} w_{V_{fi}}\right)^2 + \left(\frac{\partial \mathrm{Re}}{\partial D_i} w_{D_i}\right)^2 + \left(\frac{\partial \mathrm{Re}}{\partial \nu_a} w_{\nu_a}\right)^2}$$

Air Side Reynolds Number Uncertanity Calculation

$$\mathrm{Re} = \frac{V_{air,\max} D_o}{\nu_a}$$

$$\mathrm{Re}_a = \mathrm{Re}_a(V_{air,\max} D_o, \nu_a)$$

$$\mathrm{Re}_a = \sqrt{\left(-\frac{\partial \mathrm{Re}_a}{\partial V_a} w_{V_{ai}}\right)^2 + \left(\frac{\partial \mathrm{Re}_a}{\partial D_i} w_{D_i}\right)^2 + \left(\frac{\partial \mathrm{Re}_a}{\partial \nu_a} w_{\nu_a}\right)^2}$$

Fluid Side Uncertanity Calculation

$$Nu = \frac{\frac{f}{8}\mathrm{Re}_f \,\mathrm{Pr}(T)}{1 + 12.7\frac{f}{8}^{0.5}(\mathrm{Pr}(T)^{2/3} - 1)} + \left[1 + \left(\frac{d_i}{l}\right)^{2/3}\right]$$

Tablo 4.2-1 : Uncertanity Values.

Calculation Parameters	Average Uncertanity Value(%)
Fluid side Heat Capacity	2.26
Air side Heat Capacity	5.26
Fluid side Reynolds number	2.06
Air side Reynolds number	3.2
Overall Heat Transfer coefficient	2.6
Fluid side heat transfer coefficient	2.3
Air side heat transfer coefficient	3.6
Colburn j-factor	3.4

CURRICULUM VITAE

Name Surname **:** Oğuz KILIÇ

EDUCATION **:**

- **B.Sc.** **:** 2020, Kocaeli University, Faculty of Engineering , Mechanical Engineer